NASA CONTRACTOR REPORT

NASA CR-2390

NASA CR-2390

THEORETICAL STUDY OF THE EFFECTS OF REFRACTION ON THE NOISE PRODUCED BY TURBULENCE IN JETS

by E. W. Graham and B. B. Graham

Prepared by
GRAHAM ASSOCIATES
Shaw Island, Wash. 98286
for Langley Research Center

NATIONAL AERONAUTICS AND SPACE ADMINISTRATION • WASHINGTON, D. C. • MARCH 1974

1. Report No.	2. Government Accession No.	3. Recipient's Catalog No.
NASA CR-2390		

4. Title and Subtitle	5. Report Date
THEORETICAL STUDY OF THE EFFECTS OF REFRACTION ON THE NOISE PRODUCED BY TURBULENCE IN JETS	March 1974
	6. Performing Organization Code
7. Author(s)	8. Performing Organization Report No.
E. W. Graham and B. B. Graham	
	10. Work Unit No.
9. Performing Organization Name and Address	
Graham Associates Shaw Island, Washington 98286	11. Contract or Grant No. NAS1-11533
	13. Type of Report and Period Covered Contractor Report
12. Sponsoring Agency Name and Address NASA Headquarters Washington, D.C. 20546	14. Sponsoring Agency Code

15. Supplementary Notes

This is a final report.

16. Abstract

The production of noise by turbulence in jets is an extremely complex problem. One aspect of that problem, the transmission of acoustic disturbances from the interior of the jet through the mean velocity profile and into the far field is here studied in detail. The jet (two-dimensional or circular cylindrical) is assumed infinitely long with mean velocity profile independent of streamwise location. The noise generator is a sequence of transient sources drifting with the surrounding fluid and confined to a short length of the jet.

The analysis can be made with some precision and few assumptions. Nevertheless the results obtained are often not evident by intuition and should be of assistance in formulating more comprehensive theories of jet noise. Two results serve as examples:

(1) If the disturbances produced locally by an acoustical source are labeled as true sound and pseudo-sound, then at a Mach number as low as 0.3 most of the far-field noise originates as pseudo-sound at the source. In contrast to this at a Mach number of zero all far-field noise originates as true sound at the source. Thus the nature of noise generation changes significantly within this small Mach number range.

(2) It is often assumed that jet noise is characterized by quadrupole type radiation. In our analysis the elimination of monopole and dipole radiation by elementary reasoning does not apply. In fact it appears that the dominance of quadrupole radiation is a characteristic of the simplified model used by Lighthill, and is not necessarily to be expected in real jets.

17. Key Words (Suggested by Author(s))	18. Distribution Statement
Jet Noise Refraction Convected Wave Equation Turbulence	Unclassified - Unlimited Cat. 02

19. Security Classif. (of this report)	20. Security Classif. (of this page)	21. No. of Pages	22. Price
Unclassified	Unclassified	102	$4.25

ERRATA

NASA Contractor Report CR-2390

THEORETICAL STUDY OF THE EFFECTS OF REFRACTION ON THE NOISE PRODUCED BY TURBULENCE IN JETS

By E. W. Graham and B. B. Graham
March 1974

The attached pages should be substituted for the corresponding pages in this report, which did not reproduce clearly.

In addition, it should be noted that the plots of far-field mean-square pressure (figs. 5 to 7, 11 to 22, 24, and 25) are polar plots with the scale given on the horizontal axis.

Issued March 1976

NOMENCLATURE*

A	Source strength coefficient
b	Slope of velocity profile in shear layer, dU/dz or dU/dr
B	$(b/\omega)K_1$ in Cartesian coordinates, or
	$(b/\omega)K$ in cylindrical coordinates
c	Speed of sound
f	First solution of ordinary differential equation in shear layer
g	Second (independent) solution
i	$\sqrt{-1}$
k(z)	Adiabatic constant for given z
k_1	Wave number in x-direction (Cartesian coordinates)
k_2	Wave number in y-direction (Cartesian coordinates)
k	Wave number = $\sqrt{k_1{}^2+k_2{}^2}$ (Cartesian coordinates);
	Wave number in axial direction (cylindrical coordinates)
K_1	Reduced wave number in x-direction = k_1/ω' (Cartesian coordinates)
K_2	Reduced wave number in y-direction = k_2/ω' (Cartesian coordinates)
K	Reduced wave number = $k/\omega' = \sqrt{K_1{}^2+K_2{}^2}$ (Cartesian coordinates);
	Reduced wave number in axial direction = k/ω' (cylindrical coordinates)
M	Mach number (based on jet temperature unless subscript a appears)
m	an integer
n	an integer
p	Pressure

---

*The secondary symbols not appearing in this list are defined where they are introduced in the analysis.

Table of Contents

NOMENCLATURE*

A	Source strength coefficient
b	Slope of velocity profile in shear layer, dU/dz or dU/dr
B	$(b/\omega)K_1$ in Cartesian coordinates, or
	$(b/\omega)K$ in cylindrical coordinates
c	Speed of sound
f	First solution of ordinary differential equation in shear layer
g	Second (independent) solution
i	$\sqrt{-1}$
k(z)	Adiabatic constant for given z
k_1	Wave number in x-direction (Cartesian coordinates)
k_2	Wave number in y-direction (Cartesian coordinates)
k	Wave number = $\sqrt{k_1^2+k_2^2}$ (Cartesian coordinates);
	Wave number in axial direction (cylindrical coordinates)
K_1	Reduced wave number in x-direction = k_1/ω' (Cartesian coordinates)
K_2	Reduced wave number in y-direction = k_2/ω' (Cartesian coordinates)
K	Reduced wave number = k/ω' = $\sqrt{K_1^2+K_2^2}$ (Cartesian coordinates);
	Reduced wave number in axial direction = k/ω' (cylindrical coordinates)
M	Mach number (based on jet temperature unless subscript a appears)
m	an integer
n	an integer
p	Pressure

---

*The secondary symbols not appearing in this list are defined where they are introduced in the analysis.

Δp	Pressure increment from acoustic waves
$\overline{\Delta p^2}$	Mean-square pressure from acoustic waves
r	Radial cylindrical coordinate
R	Radial spherical coordinate = $\sqrt{x_2{}^2+y^2+z^2} = \sqrt{x_2{}^2+r^2}$
R^*	Hyperbolic radius = $\sqrt{x^2+(1-M_s{}^2\alpha_T)r^2}$
R	Gas constant
R.P.	Denotes "real part of"
s	Condensation
S_T	Strouhal number
T	Absolute temperature
t	Time
u	Axial velocity

$U(z)$ or $U(r)$ defines jet velocity profile

v	Lateral or tangential velocity
w	Normal or radial velocity
x	Streamwise coordinate (coordinates fixed in source)
x_2	Streamwise coordinate (coordinates fixed in ambient air)
y	Lateral coordinate
z	Normal coordinate
α_T	Ratio of jet temperature to ambient temperature
γ	Ratio of specific heats
δ	Half-width of uniform velocity region
ζ	$\omega'(z-z_s)$ when $z_s \geq z_0$; $\omega'(z-z_0)$ when $z_s \leq z_0$
η	$\omega'(r-r_s)$ when $r_s \geq r_0$; $\omega'(r-r_0)$ when $r_s \leq r_0$
Θ	Angular position in far field measured from upstream jet axis
ρ	Fluid density

ϕ	Velocity potential
ψ	Angle about x-axis (cylindrical coordinates)
ω	Generating frequency
ω'	ω/c

Subscripts

a	refers to ambient
c	refers to critical
j	refers to jet
s	refers to source

Acknowledgement

The computations for this report were done at NASA Langley Research Center. Jean Mason and William Arnold ably prepared the programs.

1. INTRODUCTION

Objectives

This analysis is not intended as a comprehensive theory for the prediction of noise produced by turbulence in jets. Instead we concentrate on one aspect of this complex problem, the transmission of acoustical disturbances from the interior of the jet through a shear layer and into the far field.* These acoustical disturbances are generated by mathematically defined point sources drifting with the local fluid. We neglect temporarily the more difficult problem of identifying these mathematical sources with the turbulence which they are intended to represent.

The problem we have formulated can be treated with some precision, and with comparatively few assumptions. In spite of these simplifications the results obtained are often not predictable by simple intuitive ideas. This is in fact the main advantage of such an approach, that, for those attempting to construct more comprehensive theories of jet noise, it should provide facts not intuitively evident.

Description of Model

The noise generator chosen is a sequence of transient sources drifting with the local fluid. The jet (either two-dimensional or circular cylindrical) extends to infinity up-

---

*This includes both "convection" and "refraction" effects which are in general inseparable.

stream and downstream, with velocity profile independent of streamwise position. Thus the large velocity gradients across the jet are accounted for, and the smaller gradients in the streamwise direction are neglected. It seems reasonable to expect that the major refraction effects will be shown by such a model.

In making this analysis we consider that turbulence ("self-noise") is the only true originator of noise, and that "shear noise", being composed of linear terms, is a part of the transmission process.

It must be emphasized that this is not a stability analysis. We deal with a distribution of turbulence in the jet which is essentially independent of time. This steady-state situation is the end result of the action of instabilities.

We then attempt to find the effect of the jet mean velocity profile on the transmission of acoustic disturbances from one element of turbulence through the jet and into the far field. The scattering effect of other elements of turbulence is neglected.

Although supersonic as well as subsonic jets can be treated by the methods discussed in this report, the supersonic cases present some anomalous features which require more careful study. The results given here are therefore confined to subsonic jets.

2. DESCRIPTION OF METHODS

Generality of Methods*

All of the tasks outlined in this report have in common certain necessary steps and concepts. The noise may be generated by sources (i.e. monopole sources), dipoles or quadrupoles. The noise generators may be on center, off center in a uniform velocity region or, in some cases, in the shear layer. Temperatures may be ambient or varying across the jet. The jet itself may be two-dimensional or circular. Still, with only minor modifications certain basic ideas apply, and we review them briefly.

For convenience we will describe the jet as being two-dimensional. The velocity profile must be independent of streamwise and lateral positions. For simplicity we will say "source", and speak of a single (constant velocity gradient) shear layer on each side of it, but other singularities can be used, and more complicated shear layers can be treated.

The Source in a Jet

It is first assumed that the pulsating source is at rest in a completely stationary homogeneous fluid of infinite extent. The origin of coordinates is fixed in the source, and the conventional wave equation applies. The velocity potential produced by the source is readily expressed as the double integral of the velocity potentials for all reduced wave numbers, K_1 and K_2 in the x (streamwise) and y (lateral) directions.

---

*See references 1-5.

This corresponds to the decomposition of the source potential into an infinite set of plane waves (and exponential disturbances).

The source and some portion of the surrounding fluid at rest must next be confined within a jet. From coordinates fixed in the source this jet is seen as shear layers flowing past on each side, and outside the shear layers the ambient fluid flowing by at a fixed velocity. (See Fig. 1.) To accomplish this insertion of the source into the jet one must add to its original velocity potential the potentials for upward-moving and downward-moving waves reflected off the shear layers. These two reflected wave amplitudes are as yet unknown.

The Shear Layers and Ambient Air

In the shear layers the conventional wave equation does not apply. The correct partial differential equation is derived, and by assuming periodic solutions in the streamwise and lateral directions an ordinary differential equation is obtained in the coordinate normal to the shear layers. The ordinary differential equation is solved by power series expansions about the singular point, and two independent solutions are obtained (in each layer) with amplitudes as yet unknown.

In the ambient air the conventional wave equation applies again (for coordinates fixed in the ambient fluid). Only outward moving waves need be considered, so (in each ambient region) one solution of unknown amplitude appears.

There are now eight unknown amplitudes to be determined and four boundaries between fluid layers. Across each of these

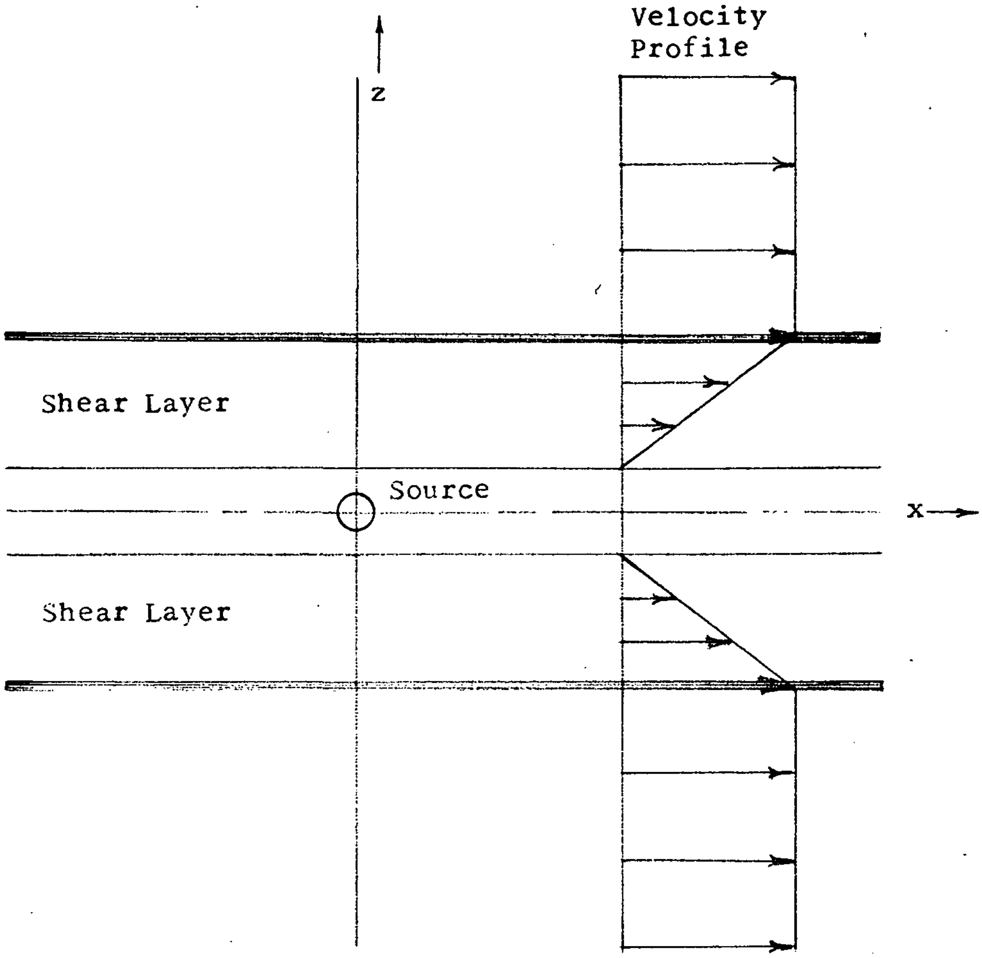

Fig. 1 COORDINATE SYSTEM FIXED IN SOURCE AND CORRESPONDING VELOCITY PROFILE

boundaries pressure and displacement must be continuous, yielding the necessary eight equations to make the system determinate. A double integral (over K_1 and K_2) for velocity potential in the ambient air is then obtained as a function of source strength and frequency.

The Far Field

Only in the far field can this double integral be evaluated easily. There the integrand generally consists of a slowly varying function multiplying a function which oscillates rapidly about zero. Such functions interact weakly, and significant contributions to the integral occur only when (a) the slowly varying function becomes rapidly varying (i.e. in the neighborhood of singular points) or (b) when the rapidly oscillating function ceases to be rapidly oscillating (i.e. in the neighborhood of stationary phase points). Evaluation of the integral yields the pressure in the far field for coordinates fixed in the source.

Transient Sources and Retarded Coordinates

A more useful result would be the far-field mean-square pressure produced by sources in a localized region, say immediately behind a jet nozzle. To obtain this we consider a sequence of transient sources, each originating at the same point relative to the ambient air or nozzle. As one source disappears after drifting downstream with the fluid, a new one (with random phase relative to the first) appears at the upstream point. The mathematical analysis of this process (Ref. 3) is rather tedious.

However the practical application conforms to a simple rule if it is assumed (as in the present analysis) that the transient sources have a lifetime of many cycles. The rule is that the mean-square pressure in source coordinates should first be formally transformed to retarded coordinates, fixed in the nozzle. (See Fig. 2.) The result must then be multiplied by $|1 + Mx_2/R|$, where M is the source Mach number relative to the ambient air, x_2 is the streamwise distance and R the radius to the far-field observation point.* (The rule holds also for the supersonic case if the $|1 + Mx_2/R|$ factors are enclosed by absolute magnitude signs.)

Contrast with Lighthill's Procedure

It may be useful to point out a few of the features in which our procedure differs from that of Lighthill[6].

In our analysis only the non-linear terms (the turbulence itself) are assumed to generate noise. All linear terms, including those commonly associated with "shear noise", are included in the transmission process.

Also, our sources are at rest in the immediately surrounding fluid and so are defined unambiguously. Lighthill's

---

* The factor $|1 + Mx_2/R|$ is often written $|1 + M \cos\Theta|$ where Θ is the angular position of the far-field observation point relative to the jet axis, $\Theta = 0$ being measured upstream, $\Theta = \pi$ downstream.

The travel distance of each transient source and the thickness of the jet are of course negligible compared to R.

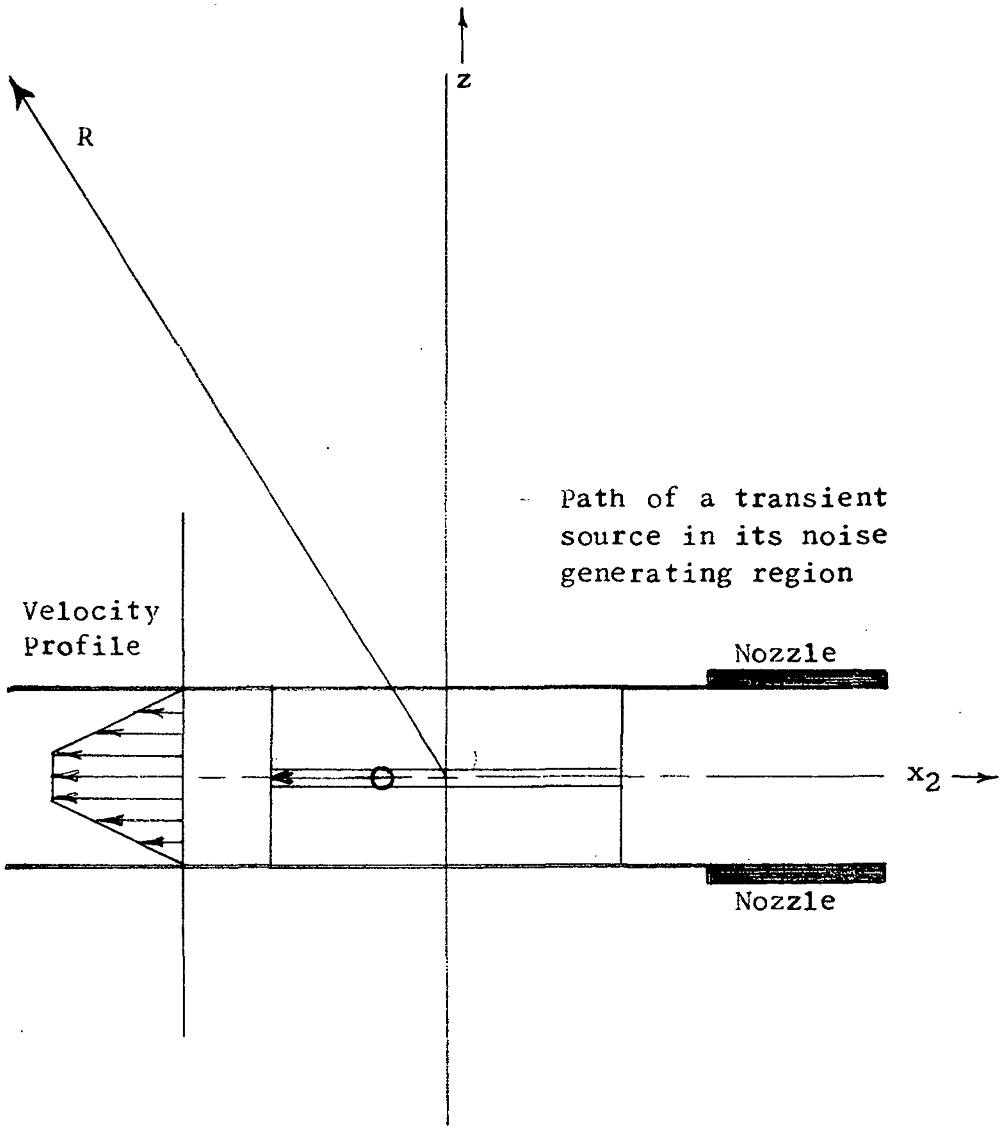

Fig. 2 COORDINATE SYSTEM FIXED RELATIVE TO NOZZLE (RETARDED COORDINATES)

sources are in motion relative to the neighboring fluid, and belong to one of the (in principle) infinitely many classes of moving sources[5].

In Lighthill's model of the noise-producing jet no fluid moves. Instead, an array of acoustical point sources passes through the fluid, all sources moving at precisely the same velocity. It is this simplification of the model which leads to the elimination of source and dipole noise, and leaves quadrupoles as the dominant noise generators in Lighthill's analysis.

3. DISCUSSION OF DIPOLES AND QUADRUPOLES

Since quadrupoles are frequently assumed to be the primary noise generators in a jet, our analyses have included such singularities located on the center-line of a two-dimensional jet (see Appendix).

However, in examining the construction of dipoles and quadrupoles in a shear layer we were led to the conclusion that there is no obvious reason for excluding the simple and highly efficient monopole source as a primary noise generator. A discussion of these ideas follows.

We visualize a dipole as being the limit approached when a source and sink* of equal strength are brought together, the strength being inversely proportional to the separation distance. In a region of uniform fluid velocity (such as assumed at the centerline) this presents no conceptual problem. The source and sink, each drifting with the fluid, travel at the same velocity and maintain the same relative positions. In a shear layer this may not be true. Both the length and direction of the line connecting source and sink may vary. One might suppose that in the limit, when source and sink coincide, this would be unimportant. However for a constant velocity gradient in the z-direction the percentage change in length and the rotation of the axis are independent of the z displacement, and may be 40 percent and 90 degrees, respectively, when source and sink travel one jet diameter (or less). Another, and possibly more important, problem is that the faster moving

---

* a pulsating source 180-degrees out of phase

source generally produces much greater pressures in the far field. As the source and sink approach each other this effect might be lost except that their strengths are being increased in the process of dipole construction. To illustrate this possibility we consider $d(\phi_s)/dz$ as compared to $d(z\phi_s)/dz$, where ϕ_s is source potential and $z\phi_s$ crudely weights the effective strength for radiation. The former is proportional to the potential of an ordinary dipole, but the latter contains a residual source potential.

What we now suggest is that the absence of any net source strength in the entire jet does not necessarily result in purely dipole radiation, nor does the absence of a net dipole strength result in purely quadrupole radiation in our analysis. Thus one of the commonly used arguments in the exclusion of source and dipole radiation apparently does not apply here. There may be other and better reasons for choosing quadrupoles in some instances. Until these are clarified, however, we propose to deal with the simpler source noise generation in the subsequent tasks of this study.

4. THE SOURCE IN THE SHEAR LAYER OF A TWO-DIMENSIONAL JET

A. DEVELOPMENT OF EQUATIONS

Symmetric and Anti-Symmetric Solutions

To analyze the case of a source located in the shear layer of a jet (Fig. 3), we first assume a narrow region (width 2δ) of uniform velocity (U_s) within the shear layer. The source is located in this uniform-velocity region, and is traveling with it, so that *the source is at rest relative to the immediately* surrounding fluid. In a coordinate system moving with the source the jet velocity distribution is then as sketched in Fig. 4. This problem can be solved by the methods briefly outlined in Section 2. The thickness of the uniform-flow region is then allowed to approach zero.

In order to reduce the number of simultaneous equations to be solved we utilize in practice the properties of symmetrical and anti-symmetrical solutions. First, we assume two sources symmetrically disposed about the centerline of the jet and pulsating exactly in phase. This problem is completely symmetrical and can be solved in the half-jet by requiring no displacement at the centerline. Next, the anti-symmetrical problem is solved considering the symmetrically disposed sources to be pulsating 180-degrees out of phase. This problem is also solved in the half-jet, but using zero pressure at the jet centerline. The superposition of velocity potentials for these two cases gives

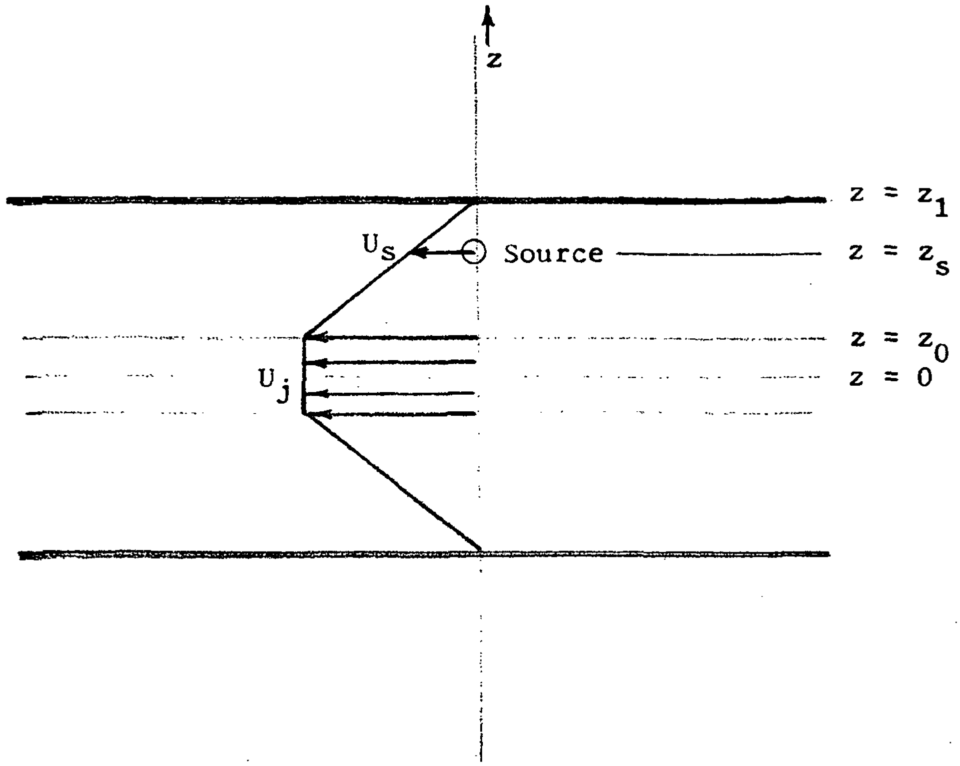

Fig. 3 TWO-DIMENSIONAL JET WITH SOURCE IN SHEAR LAYER

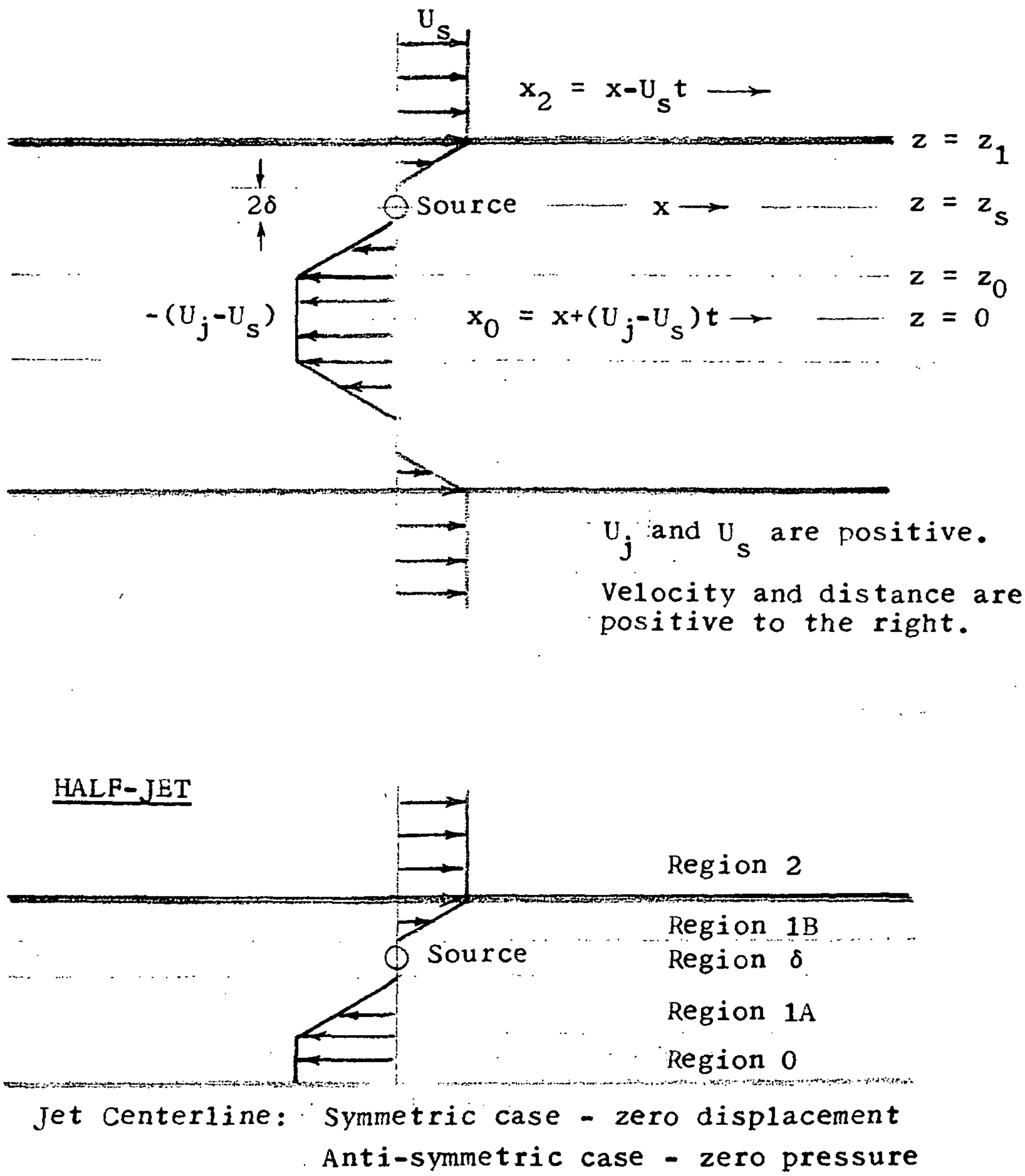

Fig. 4 JET GEOMETRY AND VELOCITY PROFILE

(Coordinates Fixed in Source)

the result for a single source (of double strength). The mean-square pressure is then found for a single source of the proper strength.

Since the jet is symmetrical we can expect, on the average, to find a similar source on the opposite side of the jet, but with random phase relative to the first source, and we add their mean-square pressures. (Note that the earlier use of in-phase and out-of-phase source pairs was a purely mathematical expedient for constructing a single source on one side of the jet.)

Coordinate Systems

The basic coordinate system (x,y,z) is fixed in the source, with x the streamwise, y the lateral and z the normal coordinate. Coordinates fixed in the ambient air are x_2,y,z, and those fixed in the uniform flow region at the jet center are x_0,y,z, where

$$\begin{aligned} x_2 &= x-U_s t \\ x_0 &= x+(U_j-U_s)t \end{aligned} \tag{1}$$

Here U_s and U_j are, respectively, the absolute magnitudes of the source and jet velocities relative to the ambient air, and t is time.

The Central Uniform-Flow Region

In Region 0 (see Fig. 4) the flow is uniform, and the conventional wave equation is satisfied in coordinates fixed in the fluid:

$$\phi_{x_0x_0} + \phi_{yy} + \phi_{zz} - (1/c^2)\phi_{tt} = 0 \tag{2}$$

where ϕ is the velocity potential, c is the speed of sound and t is time.

To satisfy the wave equation, provide for upward- and downward-moving waves and satisfy the condition of zero displacement (or zero pressure) at the jet centerline we choose ϕ_0 to be

$$\phi_0 = A\omega' \text{ R.P. } \overline{R}\left\{\exp\left[i\,\omega'(K_1x+K_2y-ct+z\sqrt{[1+K_1(M_j-M_s)]^2-K^2}\,)\right] \right.$$
$$\left. \begin{smallmatrix}+\\(-)\end{smallmatrix}\ \exp\left[i\,\omega'(K_1x+K_2y-ct-z\sqrt{[1+K_1(M_j-M_s)]^2-K^2}\,)\right]\right\} \tag{3}$$

where $x = x_0-(U_j-U_s)t$. As mentioned earlier we are dealing with two cases here. The symmetric case represents a source at $z = z_s$ and a source at $z = -z_s$, and in the half-jet at $z = 0$ there is required

$$(\partial\phi_0/\partial z) = 0 \tag{4}$$

The anti-symmetric case represents a source at $z = z_s$ and a "sink" at $z = -z_s$, and in the half jet at $z = 0$

$$(\partial\phi_0/\partial t)_{x_0=\text{const.}} = 0 \qquad (5)^*$$

This latter case is indicated by the minus sign in parentheses before the second term of Eq. (3).

In Eq. (3), $A = (\text{source strength})/8\pi^2$, the source strength being the maximum volume introduced per unit time. $\omega' = \omega/c$ where ω is the generating frequency in radians per second and

---

*pressure $(\Delta p) = -\rho\phi_{0_t} = -\rho(\partial\phi_0/\partial t)_{x_0=\text{const.}}$

c is the speed of sound. $\overline{R}$ is a complex reflection coefficient, $\overline{R} = R' + iR''$. $K_1 = k_1/\omega'$, $K_2 = k_2/\omega'$, $K^2 = K_1^{\,2} + K_2^{\,2}$. k_1 and k_2 are respectively the wave numbers in the x and y directions. M_j is the maximum jet Mach number ($M_j = U_j/c$) and M_s is the source Mach number ($M_s = U_s/c$). R.P. denotes "the real part of". (The jet is here assumed to be at ambient temperature, so that ρ and c retain constant values throughout the flow field.)

The Source Region and the Ambient Air

In Region δ (see Fig. 4) we have

$$\begin{aligned}\phi = A\omega' \; R.P. \Big\{ & \exp\left[i\omega'(K_1x+K_2y-ct+|z-z_s|\sqrt{1-K^2}\,)\right]/\sqrt{1-K^2} \\ & + \overline{P}\exp\left[i\omega'(K_1x+K_2y-ct-z\sqrt{1-K^2}\,)\right]/\sqrt{1-K^2} \\ & + \overline{J}\exp\left[i\omega'(K_1x+K_2y-ct+z\sqrt{1-K^2}\,)\right]/\sqrt{1-K^2}\Big\} \end{aligned} \tag{6}$$

where the first term, integrated from $-\infty$ to $+\infty$ in both K_1 and K_2, gives the potential for a source in a homogeneous fluid of infinite extent. The second and third terms account for downward and upward moving waves reflected off the boundaries of the δ-region. $\overline{P}$ and $\overline{J}$ are respectively $P'+iP''$ and $J'+iJ''$, complex reflection coefficients.

In region 2 (Fig. 4), the ambient air, we have

$$\phi_2 = A\omega' \; R.P. \; \overline{S}\exp\left\{i\omega'\left[K_1(x_2+U_st)+K_2y-ct\pm(z-z_1)\sqrt{(1-K_1M_s)^2-K^2}\right]\right\} \tag{7}$$

where the lower sign is used for reversed waves ($c-K_1U_s < 0$ and $(1-K_1M_s)^2 > K^2$). Otherwise the upper sign is used (ordinary waves when $c-K_1U_s > 0$ and $(1-K_1M_s)^2 > K^2$; exponential decay when

$(1-K_1M_s)^2 < K^2$). $\overline{S}$ is a complex transmission coefficient here defined as $\overline{S} = S'+iS''$ for convenience in satisfying boundary conditions in complex form. (In some of our previous analyses $\overline{S}$ was defined as $S''-iS'$, but this change causes no confusion in the final result where only $S'^2+S''^2$ appears.)

The Shear Layer Regions

So far we have considered only the regions of uniform flow. The shear layer regions must be treated differently, using s, the condensation, and w, the vertical velocity, instead of the velocity potential ϕ. The conventional wave equation is replaced by a more complicated form[1] which, upon the assumption of simple harmonic forms in the x and y directions, yields an ordinary differential equation (Eq. (17), given later) in the z (or ζ) direction.

In Region 1B (see Fig. 4)

$$s = \text{R.P. } \overline{Q}_B(\zeta_B) \exp\left[i\omega'(K_1x+K_2y-ct)\right] \tag{8}$$

$$w = \text{R.P. } \left[-ic/(1-B\zeta_B)\right] \overline{Q}_{B_\zeta} \exp\left[i\omega'(K_1x+K_2y-ct)\right] \tag{9}$$

where

$$B = (b/\omega)K_1 \text{ and } b = dU/dz \tag{10}$$

U is the local shear velocity in the layer. ζ_B is a coordinate in the z direction defined by

$$\zeta_B = \omega'\left[z - (z_s+\delta)\right] \tag{11}$$

$\overline{Q}_B$ is a complex function of ζ_B and $\overline{Q}_{B_\zeta}$ is the derivative of this function with respect to ζ_B. (Note that $\overline{R}$, $\overline{P}$, $\overline{J}$ are complex coefficients but independent of the z (or ζ) coordinate.)

$\overline{Q}_B$ is composed of solutions of the ordinary differential equation which applies in a shear layer (Eq. (17)) as will be indicated later.

In Region 1A, similarly,

$$s = \text{R.P. } \overline{Q}_A(\zeta_A) \exp\left[i\,\omega'(K_1x+K_2y-ct)\right] \tag{12}$$

$$w = \text{R.P. } \left[-ic/(1-B\zeta_A)\right] \overline{Q}_{A_\zeta} \exp\left[i\,\omega'(K_1x+K_2y-ct)\right] \tag{13}$$

where ζ_A is a coordinate in the z direction defined by

$$\zeta_A = \omega'\left[z - (z_s - \delta)\right] \tag{14}$$

Now, if $\delta \to 0$, $\zeta_A \to \zeta_B \to \zeta$, where

$$\zeta = \omega'(z-z_s) \tag{15}$$

We may write

$$\begin{aligned} \overline{Q}_A &= \overline{a}_A\, f(\zeta) + \overline{b}_A\, g(\zeta) \\ \overline{Q}_B &= \overline{a}_B\, f(\zeta) + \overline{b}_B\, g(\zeta) \end{aligned} \tag{16}$$

where $f(\zeta)$ and $g(\zeta)$ are solutions of the shear layer differential equation[1]

$$(1-B\zeta)F_{\zeta\zeta} + 2BF_\zeta + (1-B\zeta)\left[(1-B\zeta)^2 - K^2\right]F = 0 \tag{17}$$

and $\overline{a}_A$, $\overline{b}_A$, $\overline{a}_B$, $\overline{b}_B$ are complex coefficients to be determined by the boundary conditions.

$f(\zeta)$ and $g(\zeta)$ have the forms[1]

$$f(\zeta) = \sum_{n\ \text{even}} C_n\ (1-B\zeta)^n\ , \quad C_0 = 1 \tag{18}$$

$$g(\zeta) = \sum_{n\ \text{odd}} C_n\ (1-B\zeta)^n\ , \quad C_1 = 0,\ C_3 = 1$$

where

$$C_n = \frac{K^2\ C_{(n-2)} - C_{(n-4)}}{n(n-3)B^2} \tag{19}$$

The Boundary Conditions

At the jet centerline we have already provided for applying the condition of zero normal displacement (symmetrical case) or zero pressure (anti-symmetrical case). Across each interface between two regions the pressure, Δp, and the normal velocity*, w, must be continuous. (In uniform-flow regions $w = \phi_z$ and $\Delta p = -\rho\phi_t$, with coordinates fixed in the fluid. In shear layers w is given previously and $\Delta p = \rho c^2 s$.)

The application of these boundary conditions and the solution of the resulting set of simultaneous equations is a tedious but straight-forward process. Only the results are given here.

The Transmission Coefficients and Final Results

The transmission coefficients may be written

---

*More precisely the normal displacement must be continuous, but where there are no discontinuities in streamwise velocity, as in this case, normal velocity is also correct.

$$S'' = \frac{-2(1-K_1M_s)\left[f(0)[\;]_g - g(0)[\;]_f\right]\left[f_\zeta(\zeta_1)[\;]_g - g_\zeta(\zeta_1)[\;]_f\right]}{\text{Den.}}$$

$$S' = \frac{\pm 2(1-K_1M_s)\sqrt{(1-K_1M_s)^2-K^2}\left[f(0)[\;]_g - g(0)[\;]_f\right]}{\text{Den.}} \;\cdot$$

$$\cdot\left[f(\zeta_1)[\;]_g - g(\zeta_1)[\;]_f\right] \tag{20}$$

where in the symmetric case ($S' = S_s'$, $S'' = S_s''$)

$$\begin{aligned} [\;]_g &= g_\zeta(\zeta_0)\cos\sigma_0 + \sqrt{[1+K_1(M_j-M_s)]^2-K^2}\,\sin\sigma_0\, g(\zeta_0) \\ [\;]_f &= f_\zeta(\zeta_0)\cos\sigma_0 + \sqrt{[1+K_1(M_j-M_s)]^2-K^2}\,\sin\sigma_0\, f(\zeta_0) \end{aligned} \tag{21}$$

and in the anti-symmetric case ($S' = S_a'$, $S'' = S_a''$)

$$\begin{aligned} [\;]_g &= g_\zeta(\zeta_0)\sin\sigma_0 - \sqrt{[1+K_1(M_j-M_s)]^2-K^2}\,\cos\sigma_0\, g(\zeta_0) \\ [\;]_f &= f_\zeta(\zeta_0)\sin\sigma_0 - \sqrt{[1+K_1(M_j-M_s)]^2-K^2}\,\cos\sigma_0\, f(\zeta_0) \end{aligned} \tag{22}$$

and where

$$\begin{aligned} \zeta_1 &= \zeta(z=z_1) = M_s\omega/b \\ \zeta_0 &= \zeta(z=z_0) = -\omega(M_j-M_s)/b \end{aligned} \tag{23}$$

$$\sigma_0 = \omega' z_0\sqrt{[1+K_1(M_j-M_s)]^2-K^2} \tag{24}$$

$$\begin{aligned} \text{Den.} = &\left[f_\zeta(\zeta_1)[\;]_g - g_\zeta(\zeta_1)[\;]_f\right]^2 \\ &+ \left[(1-K_1M_s)^2-K^2\right]\left[f(\zeta_1)[\;]_g - g(\zeta_1)[\;]_f\right]^2 \end{aligned} \tag{25}$$

(The sign choice in S' corresponds to the sign choice in Eq. (7).)

Application of the far-field analysis (using the principle of stationary phase) and transformation to retarded coordinates gives the critical K values as

$$K_1 = \frac{x_2/R}{1+M_s x_2/R}$$
$$K_2 = \frac{y/R}{1+M_s x_2/R} \qquad (26)$$

where x_2, y, z (and $R = \sqrt{x_2^2+y^2+z^2}$) are the retarded coordinates fixed in the nozzle*.

From the far-field potential for a permanent source of frequency ω (the case so far considered), the far-field potential for the transient source sequence described previously (Section 2) can be obtained by methods derived in Ref. 4. The final result for mean-square pressure in the far field, assuming each transient source goes through 2n cycles of frequency ω_0, is[4]

$$\overline{\Delta p^2} = \frac{2A^2\rho^2\omega_0^2}{R^2}\,\frac{z^2}{R^2}\,\frac{\pi^2}{\left|1+Mx_2/R\right|^5} \cdot$$

$$\cdot\ \frac{2}{\pi^2 n}\int_0^\infty \frac{(\omega/\omega_0)^2\ (S'^2+S''^2)\ \sin^2(2\pi n\omega/\omega_0)\ d(\omega/\omega_0)}{\left[(\omega/\omega_0)^2 - 1\right]^2} \qquad (27)$$

or, if each transient source is assumed to go through many cycles,

$$\overline{\Delta p^2} = \frac{2\pi^2A^2\rho^2\omega_0^2}{R^2}\,\frac{z^2}{R^2}\,\frac{\left[S'^2(\omega_0) + S''^2(\omega_0)\right]}{\left|1+Mx_2/R\right|^5} \qquad (28)$$

---

*The nozzle is here assumed to be stationary in the ambient air.

In these equations $S' = \frac{1}{2}(S_s'+S_a')$, $S'' = \frac{1}{2}(S_s''+S_a'')$, subscripts s and a denoting values found from Eqs. (20) for the symmetric and anti-symmetric problems, respectively. The result is the mean-square pressure for a single off-center source of strength $8\pi^2 A$. M is the source Mach number (M_s). (For a single source on the far side of the jet, the mean-square pressure is given by Eq. (27) or Eq. (28) with $S' = \frac{1}{2}(S_s'-S_a')$, $S'' = \frac{1}{2}(S_s''-S_a'')$.)

Henceforth, for convenience we drop the subscript 0 on the generating frequency which will be designated simply ω. This should cause no confusion.

Special Case: Source in Central Uniform-Flow Region

The special case of a source at the center of a shear layer jet has been treated in detail in earlier work[2,3]. If the source is not on the centerline but is in the uniform-flow region inside the shear layers, the analysis is similar. There is no need to consider the special δ-region introduced when the source is in the shear layer, and the component source solution (i.e. the first term of Eq. (6)) is added to the central region potential in Eq. (3) , where now $M_s = M_j$. In the shear layer we define

$$\zeta = \omega'(z-z_0) \tag{29}$$

(replacing the previous Eq. (15)), so that in the definitions of Eqs. (21)-(25) we have

$$\begin{aligned} \zeta_0 &= 0 \\ \sigma_0 &= \omega' z_0 \sqrt{1-K^2} \\ M_s &= M_j \end{aligned} \tag{30}$$

The transmission coefficients reduce, in the symmetric case, to

$$S_s' = \mp 2\cos\sigma_s \frac{3B(1-M_sK_1)\sqrt{(1-M_sK_1)^2-K^2}\left[f(\zeta_1)[\ ]_g-g(\zeta_1)[\ ]_f\right]}{\text{Den.}}$$

$$S_s'' = 2\cos\sigma_s \frac{3B(1-M_sK_1)\left[f_\zeta(\zeta_1)[\ ]_g-g_\zeta(\zeta_1)[\ ]_f\right]}{\text{Den.}}$$

(31)

where

$$\sigma_s = \omega' z_s \sqrt{1-K^2} \qquad (32)$$

and $[\ ]_f$, $[\ ]_g$ are defined in Eqs. (21) (with $\zeta_0 = 0$). For the anti-symmetric transmission coefficients, $\cos\sigma_s$ is replaced by $\sin\sigma_s$ and $[\ ]_f$, $[\ ]_g$ are of course given by Eqs. (22).

B. DISCUSSION OF COMPUTED RESULTS FOR SOURCES OFF THE CENTERLINE

Typical Examples (for $M_j = 0.7$)

Fig. 5 illustrates the effect of moving a source off the centerline within the central uniform-velocity region of the jet. The greatest mean-square pressure occurs when the source is on the "near" side (nearest the side on which the measurement is made). However the variation is small, and the average of near and far side sources (shown in Fig. 6) is negligibly different from a source on the centerline. These results are for a Strouhal number of 0.2, and would not necessarily hold for Strouhal numbers of 1.0 or 2.0.

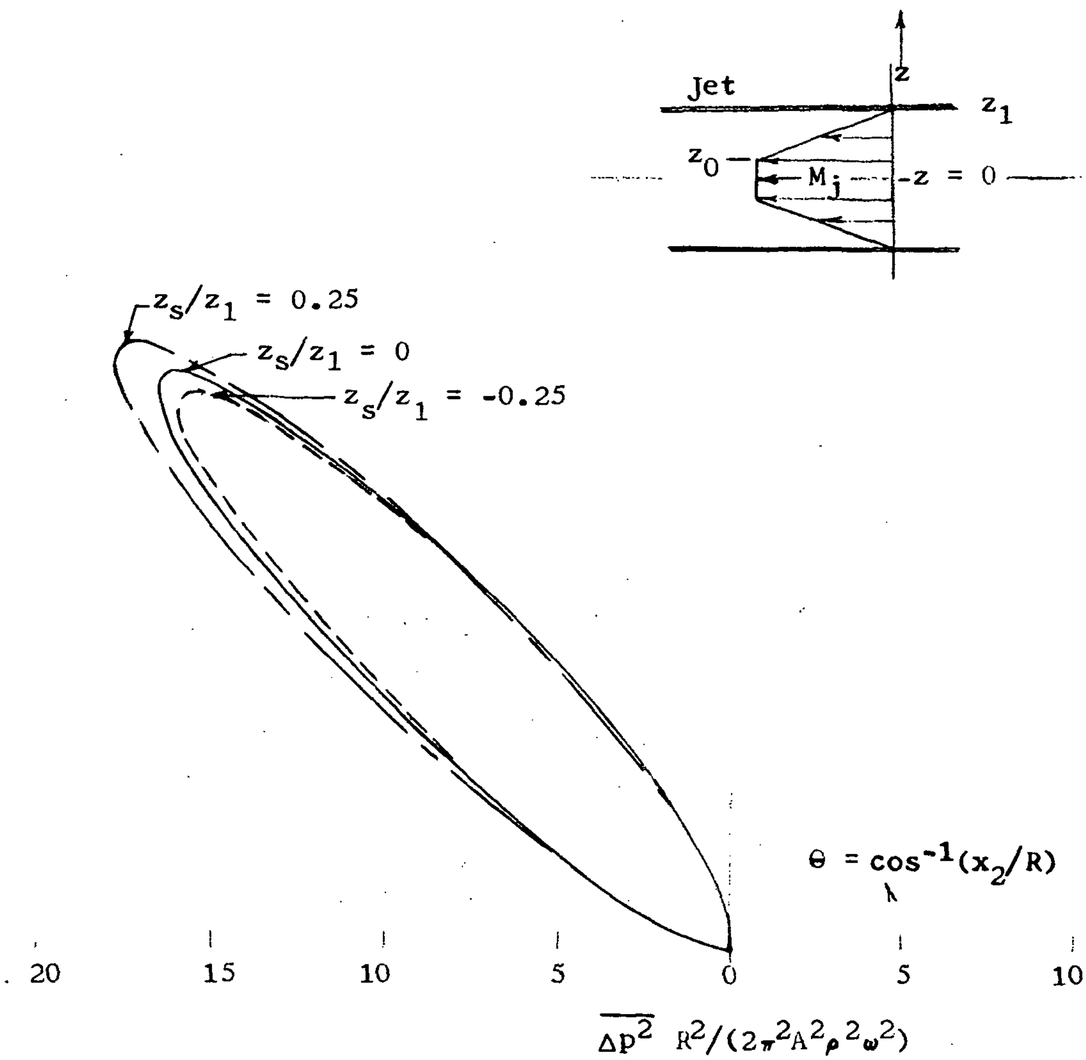

Fig. 5 POLAR PLOT OF FAR-FIELD MEAN-SQUARE PRESSURE FOR THREE SOURCE POSITIONS IN THE UNIFORM-VELOCITY PART OF THE JET (Two-Dimensional Jet, $M_j = 0.7$, $S_T = 0.2$, $z_0/z_1 = 0.25$)

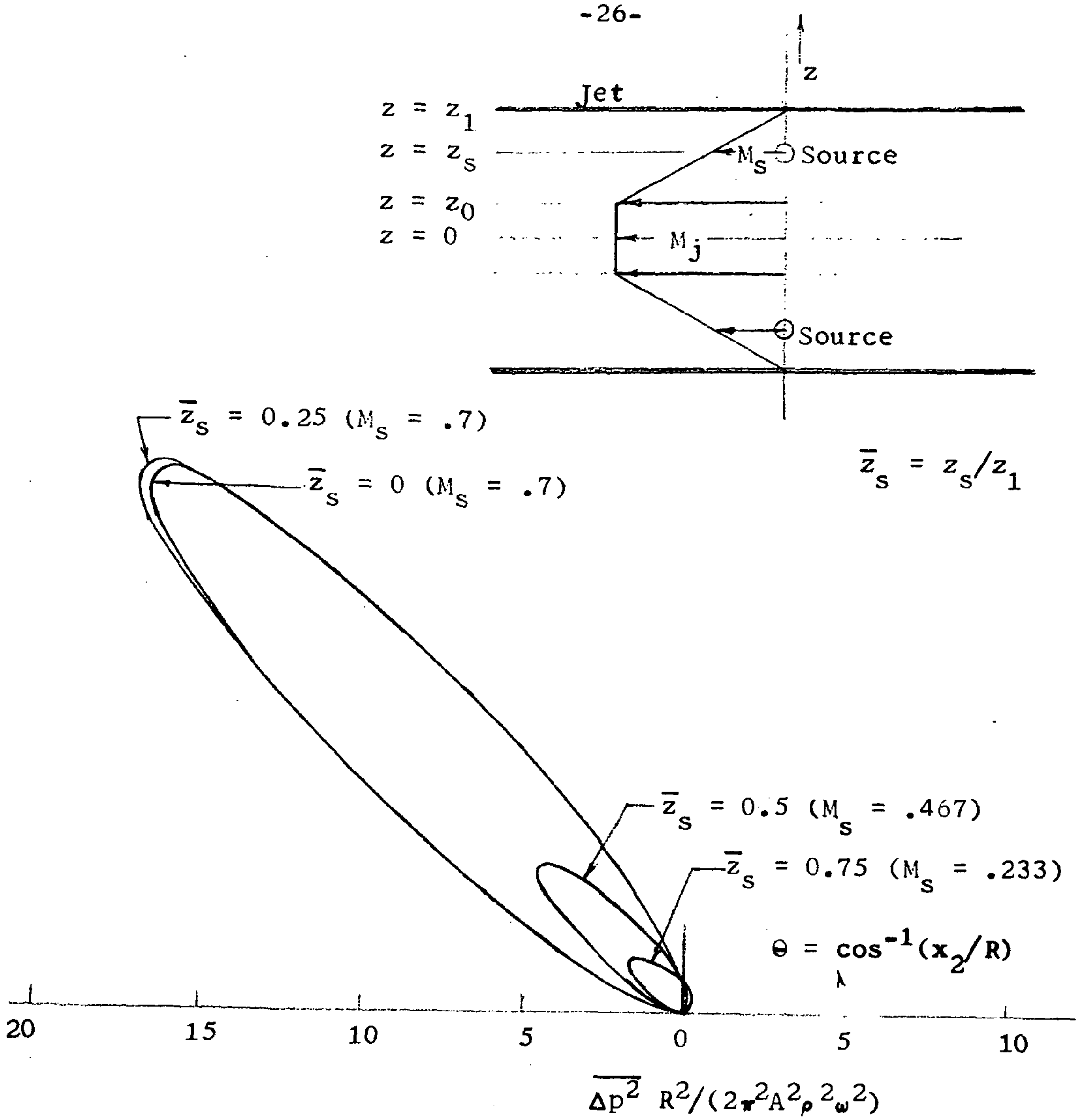

Fig. 6 FAR-FIELD MEAN-SQUARE PRESSURE FOR SEVERAL SOURCE POSITIONS IN A SHEAR-LAYER JET (Two-Dimensional Jet, $M_j = 0.7$, $S_T = 0.2$, $z_0/z_1 = 0.25$.)

In Fig. 6 the central region of uniform velocity is one-quarter of the jet thickness (as in Fig. 5). However the sources are placed in the shear layer one-third and two-thirds of the way out in the linear velocity profile region. Here the far-field mean-square pressures shown are the average for a near side and a far side source, whose effects are similar at this Strouhal number of 0.2. Fig. 7 shows similar results for a source at the mid-point of the shear layer when the central uniform-velocity region covers half the jet thickness.

The most obvious conclusion to be drawn from Figs. 6 and 7 is that a source of given strength and frequency radiates much less noise when traveling at reduced velocity in the shear layer than when traveling with the central portion of the jet. If the shear layer is to compete with the central region in noise production it must contain many more or much stronger sources. This is, of course, the case where the potential-core region of the jet persists. Further downstream the central region of the jet may become important.

Residual Source and Dipole Radiation in the Present Analysis

It is also of interest to observe in Fig. 6 the sources one-third and two-thirds of the way out in the shear layer, assuming them to be 180-degrees out of phase. Such a source-sink pair could not radiate at all like a dipole because of the great difference in the magnitude of the noise radiated individually. The radiation would be primarily that of a source, and this is why we stated earlier that elementary reasoning does not appear to justify the elimination of source and dipole radiation in favor of the less efficient quadrupole radiation in this analysis.

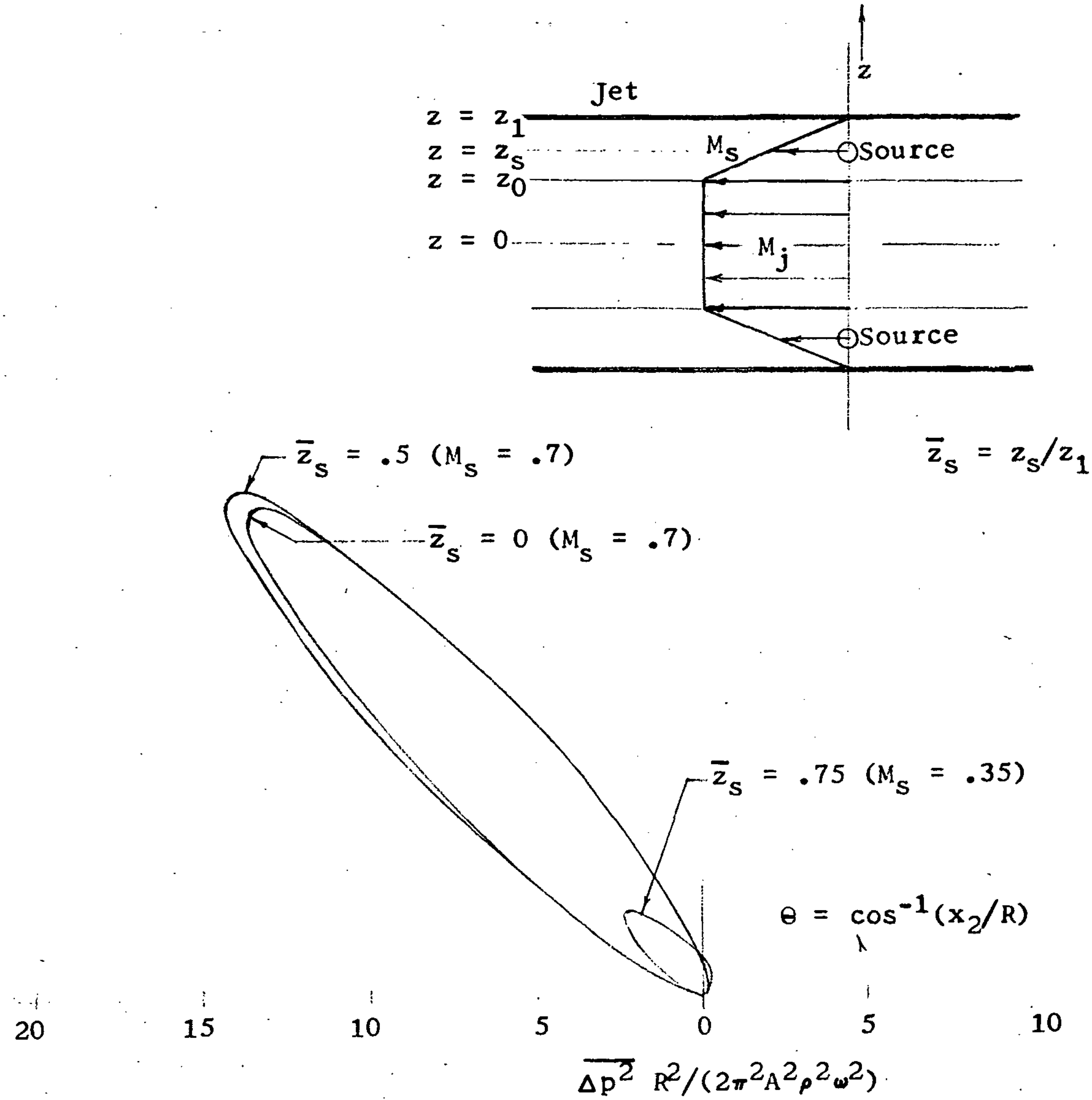

Fig. 7 FAR-FIELD MEAN-SQUARE PRESSURE FOR SEVERAL SOURCE POSITIONS IN A SHEAR-LAYER JET (Two-Dimensional Jet, $M_j = 0.7$, $S_T = 0.2$, $z_0/z_1 = 0.5$.)

Comparison with Lighthill's Analysis

The disappearance of source and dipole radiation in Lighthill's analysis is a peculiarity of the highly simplified model chosen to represent the jet. In that case the entire air mass (jet as well as ambient air) is essentially motionless, the acoustic singularities being convected, all at the same velocity, through the jet region. This means, for example, that any two sources of the same strength and frequency radiate energy to the far field in precisely the same amount and pattern except for phase. Position of the sources in the jet is unimportant for this model. Thus cancellation of the source strength causes cancellation of the source-like radiation in the far field. Similarly, cancellation of the dipole strength causes cancellation of the dipole-like radiation in the far field, leaving only quadrupole effects.

In contrast to this model, the present one puts the jet air in motion with velocity depending on the chosen velocity profile. The acoustic singularities travel with the jet air. Then two sources, for example, having the same strength and frequency generally do not radiate to the far field in the same amount and pattern. Consequently, cancellation of the source strength does not generally cancel the source-like radiation in the far field.

5. THE CIRCULAR CYLINDRICAL JET AT CONSTANT TEMPERATURE

A. DEVELOPMENT OF EQUATIONS

I. THE SHEAR LAYER

To study the transmission of acoustic disturbances through an annular fluid layer in which the velocity (U) varies with r, we start with the basic continuity equation and Euler's equation (Eqs. 1.2 and 2.3, respectively, in Landau and Lifshitz[7])

$$\frac{\partial \rho}{\partial t} + \mathrm{div}(\rho \overline{V}) = 0 \tag{33}$$

$$\frac{\partial \overline{V}}{\partial t} + (\overline{V} \cdot \mathrm{grad})\overline{V} = -\frac{1}{\rho}\,\mathrm{grad}\; p \tag{34}$$

where ρ is density, p pressure, and $\overline{V}$ is the velocity vector. In cylindrical coordinates (x,ψ,r) we will denote three mutually perpendicular velocity components as u,v,w, where u is the x-direction velocity (parallel to the axis of the jet), w is the radial (r-direction) velocity in a plane normal to the jet axis, and v is the tangential (ψ-direction) velocity in that plane. In this notation the continuity equation is written

$$\frac{\partial \rho}{\partial t} + \frac{\partial}{\partial x}(\rho u) + \frac{1}{r}\frac{\partial}{\partial \psi}(\rho v) + \frac{\partial}{\partial r}(\rho w) + \frac{\rho w}{r} = 0 \tag{33a}$$

and the three components of the Euler equation are

$$\frac{\partial u}{\partial t} + u\frac{\partial u}{\partial x} + \frac{v}{r}\frac{\partial u}{\partial \psi} + w\frac{\partial u}{\partial r} = -\frac{1}{\rho}\frac{\partial p}{\partial x}$$

$$\frac{\partial v}{\partial t} + u\frac{\partial v}{\partial x} + \frac{v}{r}\frac{\partial v}{\partial \psi} + w\frac{\partial v}{\partial r} + \frac{vw}{r} = -\frac{1}{\rho r}\frac{\partial p}{\partial \psi} \qquad (34a,b,c)$$

$$\frac{\partial w}{\partial t} + u\frac{\partial w}{\partial x} + \frac{v}{r}\frac{\partial w}{\partial \psi} + w\frac{\partial w}{\partial r} - \frac{v^2}{r} = -\frac{1}{\rho}\frac{\partial p}{\partial r}$$

Let $u = U(r) + \Delta u$, $\rho = \rho_o(1+s)$ and $p = p_o+\kappa s$, where s is the "condensation" and $\kappa = \rho_o c^2$ (see Lamb[8], pp. 476-479). (ρ_o is the density of the undisturbed fluid in the shear layer and p_0 is the mean pressure which is constant at its ambient value.) Assuming small perturbations and retaining only first-order terms, the equations of motion become

$$\Delta u_t + U(r)\,\Delta u_x + w\,U_r(r) = -\,c^2\,s_x$$

$$v_t + U(r)\,v_x = -\,c^2\,s_\psi/r \qquad (35)$$

$$w_t + U(r)\,w_x = -\,c^2\,s_r$$

$$s_t + s_x\,U(r) + \Delta u_x + \frac{v_\psi}{r} + w_r + \frac{w}{r} = 0 \qquad (36)$$

Eliminating Δu, v and w in turn gives

$$s_{ttt} + 3Us_{ttx} + 3U^2 s_{txx} + U^3 s_{xxx}$$
$$- c^2\left[(\nabla^2 s)_t + U(\nabla^2 s)_x\right] + 2U_r c^2 s_{rx} = 0 \qquad (37)$$

Let

$$s = F(r)\cos(m\psi)\,\overset{(\cos)}{\sin}(kx-\omega t) \qquad (38)$$

where k is wave number in the x-direction and ω is the frequency. The tangential wave number, m, is integral so that s is single-valued. Substituting Eq. (38) into (37) gives

$$(1-Uk/\omega)F_{\eta\eta} + \left[(2U_\eta k/\omega) + (1-Uk/\omega)/(\eta+r_o\omega')\right]F_\eta$$
$$+ (1-Uk/\omega)\left[(1-Uk/\omega)^2 - (k/\omega')^2 - m^2/(\eta+r_o\omega')^2\right]F = 0 \qquad (39)$$

where $\eta = \omega'(r-r_o)$ and $\omega' = \omega/c$.

For a linear velocity profile $U(r) = b(r-r_o)$, and if we denote $B = bkc/\omega^2 = (b/\omega)K$ where $K = k/\omega'$, the differential equation of the shear layer is

$$(1-B\eta)(\eta+r_o\omega')^2F_{\eta\eta} + (\eta+r_o\omega')\left[2B(\eta+r_o\omega') + (1-B\eta)\right]F_\eta$$
$$+ (1-B\eta)\left[(\eta+r_o\omega')^2\left\{(1-B\eta)^2 - K^2\right\} - m^2\right]F = 0 \qquad (40)$$

A solution of this equation can be obtained in the form

$$F = \sum_0^\infty C_n (1-B\eta)^n \qquad (41)$$

where, if we denote $\mu = 1+Br_o\omega'$,

$$\left.\begin{aligned} &C_0 = C_1 = C_2 = 0 \\ &C_3 \text{ is arbitrary} \end{aligned}\right. \qquad (42)$$

and

$$\begin{aligned} n(n-3)B^2\mu^2 C_n = \Big[& B^2\mu(n-1)(2n-7)\, C_{n-1} \\ & - \left\{(n-2)(n-4)B^2 - K^2\mu^2 - m^2B^2\right\} C_{n-2} \\ & - 2\mu K^2 C_{n-3} - (\mu^2-K^2)\, C_{n-4} \\ & + 2\mu\, C_{n-5} - C_{n-6}\Big] \end{aligned} \qquad (43)$$

(Note that C_n is zero if $n < 0$.)

To obtain a linearly independent second solution we set

$$F_2 = F_1 \ln\left|1-B\eta\right| + \sum_0^{\infty} A_n (1-B\eta)^n \tag{44}$$

where F_1 is the solution already obtained (Eqs. (41)-(43)) and

$$\begin{aligned}
A_0 &= 3\mu^3 B^2 C_3/(m^2B^2-K^2\mu^2) \\
A_1 &= 0 \\
A_2 &= -\ 3\mu C_3(B^2m^2+K^2\mu^2)/2(B^2m^2-K^2\mu^2) \\
A_3 &\text{ is arbitrary}
\end{aligned} \tag{45}$$

and

$$\begin{aligned}
n(n-3)\mu^2B^2 A_n = \Big[&- \mu^2B^2(2n-3)\ C_n \\
&+ \mu B^2\left\{(4n-9)\ C_{n-1} + (n-1)(2n-7)\ A_{n-1}\right\} \\
&-\ 2B^2(n-3)\ C_{n-2} - \left\{(n-2)(n-4)B^2 \right. \\
&\qquad\qquad \left. -K^2\mu^2-m^2B^2\right\} A_{n-2} \\
&-2K^2\mu\ A_{n-3} + (K^2-\mu^2)A_{n-4} \\
&+ 2\mu\ A_{n-5} - A_{n-6}\Big]
\end{aligned} \tag{46}$$

(A_n is zero if $n < 0$.)

For simplicity we designate the arbitrary constants as a,b and denote $F_1 \sim f$, $F_2 \sim g$, and write

$$F(\eta) = a\ f(\eta) + b\ g(\eta) \tag{47}$$

with

$$f(\eta) = \sum_{0}^{\infty} C_n (1-B\eta)^n \tag{48}$$

$$g(\eta) = f(\eta) \ln|1-B\eta| + \sum_{0}^{\infty} A_n (1-B\eta)^n \tag{49}$$

where $C_3 = 1$, $A_3 = 1$ and C_n, A_n as above. (b in Eq. (47) should not be confused with the slope of the velocity profile used earlier.)

Eqs. (48) and (49) express two independent solutions of the differential equation (Eq. (40)) as series expansions about the singular point $\eta = 1/B$. The series converge for those points η whose distance from $\eta = 1/B$ is less than the distance from $\eta = 1/B$ to the other singular point of the differential equation at $\eta = -\omega' r_o$. Hence these solutions may not be valid over the entire shear layer. In such cases another series solution may be obtained by expanding about some other point; we choose the outer edge of the shear layer, $\eta = \eta_1 = \omega'(r_1 - r_o)$. The convergence of this new series is then limited to those values of η which are closer to η_1 than the nearer of the two singular points of the differential equation. This solution of Eq. (40) is obtained in the form

$$F = \sum_{0}^{\infty} a_n (\eta - \eta_1)^n \tag{50}$$

a_0 and a_1 are arbitrary and, if we denote $(1-B\eta_1)/B = \nu$, $\omega' r_1 = R_1$, we obtain

$$n(n-1)\nu R_1^{\,2}\, a_n = -\Big[(n-1)R_1\{\nu(2n-3)+R_1(4-n)\}a_{n-1}$$
$$+\{(n-2)(n-3)(\nu-2R_1)+(n-2)(3R_1+\nu)$$
$$+(Q_0-\nu m^2)\}a_{n-2}$$
$$-\{(n-3)(n-5)-(Q_1+m^2)\}a_{n-3}+Q_2a_{n-4}$$
$$+Q_3a_{n-5}+Q_4a_{n-6}-B^2a_{n-7}\Big] \tag{51}$$

where

$$Q_0 = \nu R_1^{\,2}(B^2\nu^2-K^2)$$
$$Q_1 = 2R_1\nu^3B^2 - 3\nu^2B^2R_1^{\,2} - 2\nu R_1K^2 + K^2R_1^{\,2}$$
$$Q_2 = \nu^3B^2 - 6\nu^2B^2R_1 + 3\nu B^2R_1^{\,2} - \nu K^2 + 2R_1K^2 \tag{52}$$
$$Q_3 = 6\nu B^2R_1 - 3\nu^2B^2 - B^2R_1^{\,2} + K^2$$
$$Q_4 = B^2(3\nu-2R_1)$$

(a_n is zero for $n < 0$.)

In this case two independent solutions are obtained by letting first one and then the other of the arbitrary constants be zero. Thus we may write, as before,

$$F(\eta) = a\,f(\eta) + b\,g(\eta) \tag{53}$$

where a,b are arbitrary and

$$f(\eta) = \sum_0^\infty a_n\,(\eta-\eta_1)^n \qquad \text{with } a_0 = 1,\; a_1 = 0,\; a_n \text{ as given above;} \tag{54}$$

$$g(\eta) = \sum_0^\infty a_n\,(\eta-\eta_1)^n \qquad \text{with } a_0 = 0,\; a_1 = 1,\; a_n \text{ as given above.} \tag{55}$$

In some cases neither series solution (Eqs. (48) and (49) nor Eqs. (54) and (55)) is valid over the entire shear layer. One series can be applied in one part of the shear layer, however, and the other series in another part of the shear layer, and there is an overlapping region where both series are valid. In such cases the solutions must be matched at some point within this overlapping region. This is accomplished by establishing conditions of equal pressure and equal radial velocity at the matching point, so that the arbitrary constants a,b in Eq. (47) are thereby related to those in Eq. (53).

(The second singular point of the differential equation, i.e. that at $\eta = -\omega' r_o$, corresponds to $r = 0$, the center of the jet. As long as the shear layer does not extend in to the jet center (a condition which is met by the numerical examples studied later) it is not required to obtain a solution by expansion about this point. In some cases such a solution might be useful to expedite convergence, however.)

II. THE SOURCE IN A CIRCULAR SHEAR-LAYER JET

Basic Solution

In cylindrical coordinates, the wave equation governing the propagation of small disturbances in a homogeneous fluid is

$$\frac{1}{r}\frac{\partial}{\partial r}\left(r\frac{\partial \phi}{\partial r}\right) + \frac{1}{r^2}\frac{\partial^2 \phi}{\partial \psi^2} + \frac{\partial^2 \phi}{\partial x^2} = \frac{1}{c^2}\frac{\partial^2 \phi}{\partial t^2} \tag{56}$$

where ϕ is a velocity potential, c is the speed of sound and t is time. x, ψ, r are the cylindrical coordinates of a point in the homogeneous fluid.

A solution of Eq. (56) for an acoustical point source, located at the origin and at rest with respect to the fluid, is

$$\phi_s = \pi A \text{ R.P.} \int_{-\infty}^{\infty} e^{i(kx-\omega t)} H_0^{(1)}\left(r\sqrt{\omega'^2-k^2}\right) dk \tag{57}$$

where $A = (\text{source strength})/8\pi^2$, source strength being defined as maximum volume emitted per unit time, ω is the source frequency, $\omega' = \omega/c$, k is wave number in the x-direction, $H_0^{(1)}(\alpha)$ is the Hankel function of the first kind of order zero and argument α, and R.P. denotes "real part of".

Eq. (57) represents the source as a superposition over all wave numbers of cylindrical waves ($k < \omega/c$) and exponential disturbances ($k > \omega/c$).

If the source is not at the origin, but at some point $0, \psi_s, r_s$, an appropriate wave-expansion formula (see, for example, Magnus and Oberhettinger[9], p. 21, formula 3b) applied to Eq. (57) gives

$$\begin{aligned}
\phi_s &= \pi A \sum_0^{\infty} \epsilon_m \cos\left[m(\psi-\psi_s)\right] \text{ R.P.} \int_{-\infty}^{\infty} e^{i(kx-\omega t)} J_m\left(r_s\sqrt{\omega'^2-k^2}\right) \cdot \\
&\qquad \cdot H_m^{(1)}\left(r\sqrt{\omega'^2-k^2}\right) dk\,; \qquad r > r_s \\
&= \pi A \sum_0^{\infty} \epsilon_m \cos\left[m(\psi-\psi_s)\right] \text{ R.P.} \int_{-\infty}^{\infty} e^{i(kx-\omega t)} J_m\left(r\sqrt{\omega'^2-k^2}\right) \cdot \\
&\qquad \cdot H_m^{(1)}\left(r_s\sqrt{\omega'^2-k^2}\right) dk\,; \qquad r < r_s
\end{aligned} \tag{58}$$

where $\epsilon_0 = 1$, $\epsilon_m = 2$ for $m = 1,2,3,\cdots$, J_m is the Bessel function of the first kind of order m, and $H_m^{(1)}$ is the corresponding Hankel function.

Eq. (58) can be derived alternatively by representing the off-center source as a δ-function constructed by superimposing an infinite Fourier series of ring-sources, each of radius r_s and having tangentially-varying source strength proportional to $A \cos[m(\psi - \psi_s)]$. The velocity potential of the m^{th} ring-source is given by the corresponding m^{th} term of the series in Eq. (58). (Viewing the source in this manner has practical utility later on when computing the far-field pressures.)

Source in Shear Layer

To analyze the problem of a source located in the shear layer of a cylindrical jet (Fig. 8), it is convenient to first assume an annular region ($\Delta r = 2\delta$) of uniform velocity, U_s, within the shear layer. The source is located in this uniform-velocity region, and is traveling with it, so that the source is at rest relative to the immediately surrounding fluid. In a coordinate system moving with the source the jet velocity distribution is as sketched in Fig. 9. This problem can be solved, and the thickness of the annular region containing the source is then allowed to vanish ($\delta \rightarrow 0$).

Since the jet is symmetrical we can expect, on the average, to find similar sources at all angles ψ_s in the jet, but with random phase relative to each other. Their mean-square pressures are additive.

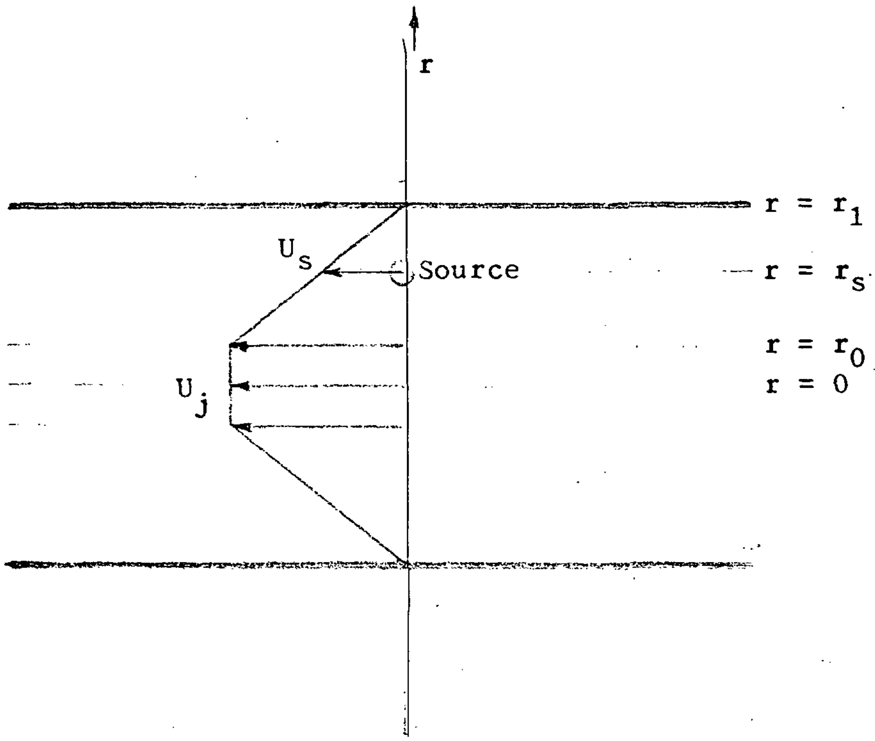

Fig. 8 STREAMWISE CROSS-SECTION OF CIRCULAR CYLINDRICAL JET WITH SOURCE IN SHEAR-LAYER, SHOWING VELOCITY PROFILE AND GEOMETRY

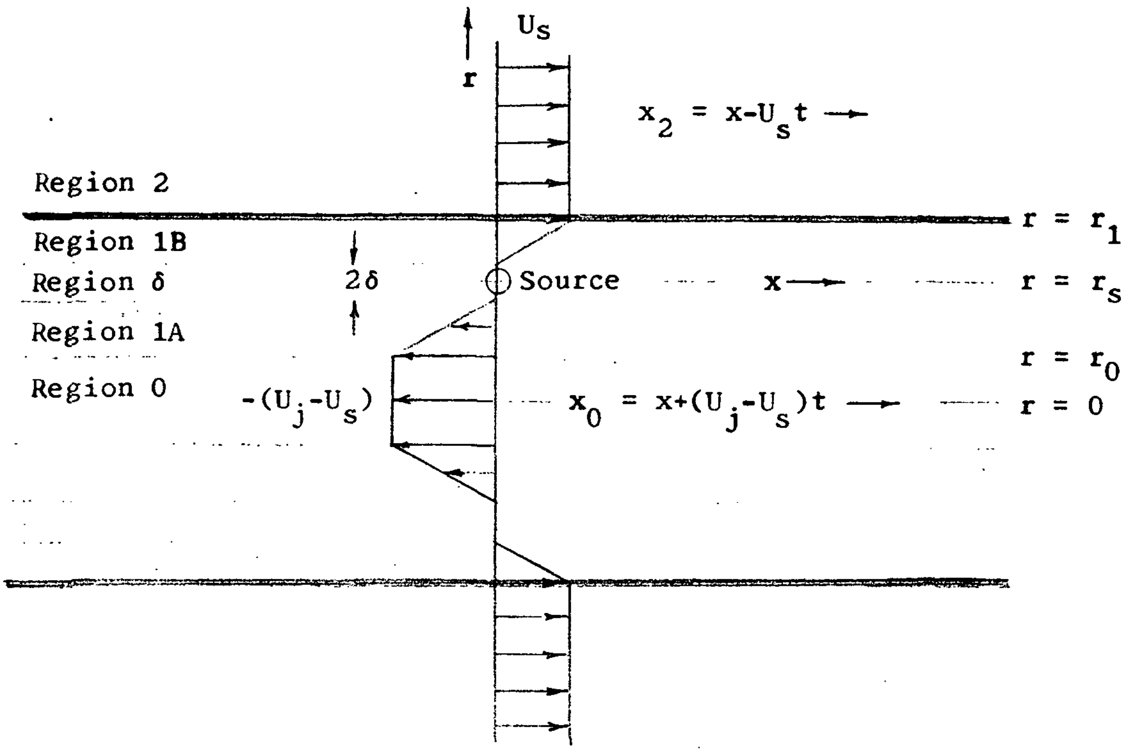

Fig. 9 JET GEOMETRY AND VELOCITY PROFILE

(Coordinates fixed in the source)

Coordinate Systems

The basic coordinate system (x,ψ,r) is fixed relative to the source, with x the streamwise coordinate parallel to the jet axis, r the radial coordinate measured from the jet centerline in planes normal to the jet axis, and ψ the angular coordinate in such planes. Coordinates fixed in the ambient air are x_2,ψ,r and those fixed in the uniform-flow region at the center of the jet are x_0,ψ,r, where

$$\begin{aligned} x_2 &= x-U_s t \\ x_0 &= x+(U_j-U_s)t \end{aligned} \qquad (59)$$

Here U_s and U_j are, respectively, the absolute magnitudes of the source and jet velocities relative to the ambient air, and t is time.

Jet Temperature and Mach Number

Most of our previous work has assumed that the jet has the same temperature as the ambient air. We now allow the jet temperature to have a different value from ambient. The jet temperature, T_j, is assumed constant throughout the jet $(r < r_1)$. Corresponding to this, the speed of sound in the jet is c_j and the density is ρ_j. Outside the jet $(r > r_1)$ the ambient air has temperature T_a, and corresponding speed of sound c_a and density ρ_a. The temperature ratio is denoted α_T:

$$\alpha_T = \frac{T_j}{T_a} = \frac{\rho_a}{\rho_j} = \left[\frac{c_j}{c_a}\right]^2 \qquad (60)$$

Although the temperature discontinuity at the outer jet boundary is unrealistic, the analysis will enable a preliminary investigation of the effects of heating the jet.

We define jet and source Mach numbers based on jet temperature:

$$\begin{aligned} M_j &= U_j/c_j \\ M_s &= U_s/c_j \end{aligned} \tag{61}$$

For convenience we define also a Mach number based on the speed of sound at ambient conditions so that

$$\begin{aligned} M_{a_j} &= U_j/c_a = \sqrt{\alpha_T}\, M_j \\ M_{a_s} &= U_s/c_a = \sqrt{\alpha_T}\, M_s \end{aligned} \tag{62}$$

The frequency parameter is

$$\begin{aligned} \omega' &= \omega/c_j \\ \omega_a' &= \omega/c_a = \sqrt{\alpha_T}\, \omega' \end{aligned} \tag{63}$$

A non-dimensional wave number is defined as

$$\begin{aligned} K &= k/\omega' \\ K_a &= k/\omega_a' = K/\sqrt{\alpha_T} \end{aligned} \tag{64}$$

The Central Uniform-Flow Region

To satisfy the wave equation, provide for outward and inward moving waves, and satisfy the condition of zero radial velocity ($\partial\phi/\partial r = 0$, i.e. no source at $r = 0$) at the jet centerline, ϕ_0 is chosen to be

$$\phi_{0_m}(K) = \pi A\omega' \epsilon_m \cos\left[m(\psi-\psi_s)\right] \ \text{R.P.}\left[\overline{R}_m \, e^{i\omega'\left[K\{x_0-(U_j-U_s)t\}-c_jt\right]} \cdot \right.$$

$$\left. \cdot \ J_m\left(r\omega'\sqrt{\left[1+K(M_j-M_s)\right]^2-K^2}\right)\right] \qquad (65a)$$

$$\phi_0 = \sum_0^{\infty} \int_{-\infty}^{\infty} \phi_{0_m}(K)\ dK \qquad (65b)$$

where $\overline{R}_m$ is a complex coefficient, $\overline{R}_m = R_m' + iR_m''$, to be determined.

Eq. (65a) is the component potential for one value of m (i.e. a single one of the source rings mentioned previously) and one value of wave number K. The total potential is obtained by integrating over all K and summing over all m, as in Eq. (65b). Since the individual component terms must each satisfy the differential equation and the boundary conditions, we will henceforth write only the component solution for each region of the flow field. The total potential is in each case the integral (over K) and the sum (over m) of the component term, as indicated for the central-region potential in Eq. (65b).

If the source is located in the central uniform-flow region, the source solution from Eq. (58) must be added to Eq. (65). For greater generality the following analysis will be applied to the case with the source in the shear layer of the jet, but the final result for the special case where $r_s < r_0$ will be given later.

The Source Region

In the annular region 8 we have

$$\phi_{\delta_m}(K) = \pi A\omega' \epsilon_m \cos[m(\psi-\psi_s)] \; R.P.\Big[\exp[i\omega'(Kx-c_jt)] \cdot$$
$$\cdot \Big\{ J_m(r_s\omega'\sqrt{1-K^2})\, H_m^{(1)}(r\omega'\sqrt{1-K^2})$$
$$+ \overline{E}_m H_m^{(1)}(r\omega'\sqrt{1-K^2}) + \overline{G}_m H_m^{(2)}(r\omega'\sqrt{1-K^2})\Big\}\Big] ;$$
$$r_s+\delta > r > r_s \qquad (66a)$$

$$= \pi A\omega' \epsilon_m \cos[m(\psi-\psi_s)] \; R.P.\Big[\exp[i\omega'(Kx-c_jt)] \cdot$$
$$\cdot \Big\{ J_m(r\omega'\sqrt{1-K^2})\, H_m^{(1)}(r_s\omega'\sqrt{1-K^2})$$
$$+ \overline{E}_m H_m^{(1)}(r\omega'\sqrt{1-K^2}) + \overline{G}_m H_m^{(2)}(r\omega'\sqrt{1-K^2})\Big\}\Big] ;$$
$$r_s > r > r_s-\delta \qquad (66b)$$

The first term in each of these equations is the m,K-component of the source potential and the other two terms account for outward and inward moving waves reflected off the boundaries of the δ-annulus. $\overline{E}_m$ and $\overline{G}_m$ are, respectively, $E_m' + iE_m''$, $G_m' + iG_m''$, complex reflection coefficients to be determined.

The first term of each of these equations, integrated over all K and summed over all m, gives the source potential which at $r = r_s$, $\psi = \psi_s$ fulfills the necessary conditions for the existence of the source. The other two terms, being the same in Eq. (66a) and in Eq. (66b), represent a solution which is continuous in both pressure and velocity across the δ-annulus. Thus the boundary conditions at $r = r_s$ are satisfied.

The Ambient Air

Outside the jet (Region 2, the ambient air, in Fig. 9) we have

$$\phi_{2_m}(K) = \pi A\omega' \epsilon_m \cos\left[m(\psi-\psi_s)\right] \; R.P.\left[\bar{S}_m \exp\left[i\omega'\{K(x_2+U_s t)-c_j t\}\right] \cdot \right.$$
$$\left. \cdot \; H_m^{(1)}\left(r\omega'\sqrt{(c_j/c_a)^2(1-KM_s)^2-K^2}\right)\right] \qquad (67)$$

where $\bar{S}_m$ is the complex transmission coefficient, $\bar{S}_m = S_m' + iS_m''$. Note that $\omega' = \omega/c_j$ and $K = k/\omega'$, as before, so that the c_j multiplying t in the exponential term is due to this definition of ω' in terms of jet temperature rather than ambient. The temperature difference effect appears in the argument of the Hankel function. That is, Eq. (67) is a solution of the local wave equation (Eq. (56), with $x = x_2$ and $c = c_a$).

When $KM_s > 1$ and $(c_j/c_a)^2(1-KM_s)^2 > K^2$, $H_m^{(1)}(\;)$ in Eq. (67) must be replaced by $H_m^{(2)}(\;)$, the Hankel function of the second kind. This is, in cylindrical coordinates, the "reversed wave" case discussed in previous reports[2].

The Shear Layer Regions

So far we have considered only the regions of uniform flow. The shear layer regions must be treated differently, using s, the condensation, and w, the radial velocity, instead of the velocity potential ϕ. The development of the shear layer equation for a circular cylindrical jet with linearly varying velocity profile was given earlier. As shown then, the conventional wave equation is replaced by a more complicated form which, upon the assumption of simple harmonic forms in the x and ψ directions, yields an ordinary differential equation (Eq. (40)) in the r (or η) direction. Two independent solutions ($f(\eta)$ and $g(\eta)$) of the shear layer equation are found by series expansion and have the forms shown previously. These are combined to give the shear-layer region solutions used below.

In Region 1B (see Fig. 9) we may write

$$s_m = \cos\left[m(\psi-\psi_s)\right] \ \text{R.P.}\left[\overline{Q}_{B_m}(\eta_B)\ e^{i\omega'(Kx-c_jt)}\right] \tag{68}$$

$$w_m = \cos\left[m(\psi-\psi_s)\right] \ \text{R.P.}\left[-\frac{ic_j}{1-B\eta_B}\ \overline{Q}_{B_{m\eta}}\ e^{i\omega'(Kx-c_jt)}\right] \tag{69}$$

where $B = (b/\omega)K$ and $b = dU/dr$. U is the local shear velocity in the layer. η_B is a coordinate in the r-direction defined by

$$\eta_B = \omega'\left[r - (r_s+\delta)\right] \tag{70}$$

$\overline{Q}_{B_m}$ is a complex function of η_B and is a combination of the solutions $f_m(\eta)$, $g_m(\eta)$ of the ordinary differential equation which applies in the shear layer. $\overline{Q}_{B_{m\eta}}$ is the derivative of $\overline{Q}_{B_m}$ with respect to η_B.

Similarly, in Region 1A (Fig. 9) we write

$$s_m = \cos\left[m(\psi-\psi_s)\right] \ \text{R.P.}\left[\overline{Q}_{A_m}(\eta_A)\ e^{i\omega'(Kx-c_jt)}\right] \tag{71}$$

$$w_m = \cos\left[m(\psi-\psi_s)\right] \ \text{R.P.}\left[-\frac{ic_j}{1-B\eta_A}\ \overline{Q}_{A_{m\eta}}\ e^{i\omega'(Kx-c_jt)}\right] \tag{72}$$

where η_A is a coordinate in the r-direction defined by

$$\eta_A = \omega'\left[r - (r_s - \delta)\right] \tag{73}$$

Now if $\delta \rightarrow 0$

$$\eta_A = \eta_B = \eta$$

$$\eta = \omega'(r - r_s) \tag{74}$$

We may write

$$\bar{Q}_{A_m} = \bar{a}_{A_m} f_m(\eta) + \bar{b}_{A_m} g_m(\eta)$$

$$\bar{Q}_{B_m} = \bar{a}_{B_m} f_m(\eta) + \bar{b}_{B_m} g_m(\eta) \tag{75}$$

where, as stated already, $f_m(\eta)$, $g_m(\eta)$ are solutions of the shear-layer equation. $\bar{a}_{A_m}$, $\bar{b}_{A_m}$, $\bar{a}_{B_m}$, $\bar{b}_{B_m}$ are complex coefficients to be determined when all the boundary conditions are satisfied.

<u>The Boundary Conditions</u>

At the jet centerline the condition of zero radial velocity has already been provided for and, similarly, at the radius of the source location, $r = r_s$, the solution was constructed to provide continuity except for the required existence of the source at $r = r_s$, $\psi = \psi_s$. Across each interface between any two of the flow regions the pressure (Δp) and the radial velocity (w) must be continuous.

In the uniform-flow regions $w = \phi_r$ and $\Delta p = -\rho_j \phi_t$ if the uniform-flow region is within the jet or $\Delta p = -\rho_a \phi_a$ outside the jet, with coordinates fixed in the local fluid in each case. In the shear-layer regions w is given previously and $\Delta p = \rho_j c_j^2 s$.

Application of the pressure and velocity boundary conditions (at the four boundaries r_0, $r_s-\delta$, $r_s+\delta$, r_1) results in a set of eight simultaneous equations to be solved for the eight unknown coefficients ($\bar{a}_{A_m}$, $\bar{b}_{A_m}$, $\bar{a}_{B_m}$, $\bar{b}_{B_m}$, $\bar{R}_m$, $\bar{S}_m$, $\bar{E}_m$, $\bar{G}_m$). Solution is tedious but straight-forward.

The Transmission Coefficient

For convenience, the following notation is used:

$$\begin{aligned} \eta_0 &= \eta(r_0) = \omega'(r_0-r_s) \\ \eta_1 &= \eta(r_1) = \omega'(r_1-r_s) \end{aligned} \tag{76}$$

$$\begin{aligned} \sigma_0 &= \omega' r_0 \sqrt{[1+K(M_j-M_s)]^2-K^2} \\ \sigma_s &= \omega' r_s \sqrt{1-K^2} \\ \sigma_1 &= \omega' r_1 \sqrt{(c_j/c_a)^2(1-KM_s)^2-K^2} \end{aligned} \tag{77}$$

$$\begin{aligned} \sqrt{1} &= \sqrt{[1+K(M_j-M_s)]^2-K^2} \\ \sqrt{2} &= \sqrt{(c_j/c_a)^2(1-KM_s)^2-K^2} \end{aligned} \tag{78}$$

Then the complex transmission coefficient is

$$\bar{S}_m = \frac{2i\ (\rho_j/\rho_a)}{\pi\omega' r_s(1-KM_s)} \; \frac{f_m(\eta_1)g_{m_\eta}(\eta_1) - g_m(\eta_1)f_{m_\eta}(\eta_1)}{f_m(0)g_{m_\eta}(0) - g_m(0)f_{m_\eta}(0)} \; \frac{[\ ]_N}{[\ ]_D} \tag{79}$$

where

$$\begin{aligned} [\ ]_N &= f_m(0)[\ ]_{g_{m0}} - g_m(0)[\ ]_{f_{m0}} \\ [\ ]_D &= [\ ]_{f_{m0}}[\ ]_{g_{m1}} - [\ ]_{g_{m0}}[\ ]_{f_{m1}} \end{aligned} \tag{80}$$

and

$$
\begin{aligned}
[\,]_{f_{m0}} &= J_m(\sigma_0) f_{m_\eta}(\eta_0) - \sqrt{\textcircled{1}}\; J_m'(\sigma_0) f_m(\eta_0) \\
[\,]_{g_{m0}} &= J_m(\sigma_0) g_{m_\eta}(\eta_0) - \sqrt{\textcircled{1}}\; J_m'(\sigma_0) g_m(\eta_0)
\end{aligned}
\tag{81}
$$

$$
\begin{aligned}
[\,]_{f_{m1}} &= H_m^{(1)}(\sigma_1) f_{m_\eta}(\eta_1) - (\rho_j/\rho_a)\sqrt{\textcircled{2}}\; H_m^{(1)}{}'(\sigma_1) f_m(\eta_1) \\
[\,]_{g_{m1}} &= H_m^{(1)}(\sigma_1) g_{m_\eta}(\eta_1) - (\rho_j/\rho_a)\sqrt{\textcircled{2}}\; H_m^{(1)}{}'(\sigma_1) g_m(\eta_1)
\end{aligned}
\tag{82}
$$

The prime following the Bessel or Hankel function indicates the derivative (e.g. $J_m'(\sigma_s) = \left[d\left\{J_m(\sigma)\right\}/d\sigma\right]_{\sigma=\sigma_s}$).

In the reversed wave case ($K > 1/M_s$ and σ_1 real), $H_m^{(1)}(\sigma_1)$, $H_m^{(1)}{}'(\sigma_1)$ are replaced by $H_m^{(2)}(\sigma_1)$, $H_m^{(2)}{}'(\sigma_1)$ in Eq. (82).

<u>Special Case: $r_s < r_0$</u>

If the source is located in the central uniform-flow region rather than in the shear layer, the preceding analysis is slightly simplified. In this case we define

$$
\eta = \omega'(r - r_0) \tag{83}
$$

Then $\eta_1 = \omega'(r_1 - r_0)$, $\eta_0 = 0$; also $\sigma_0 = \omega' r_0 \sqrt{1-K^2}$. The transmission coefficient then reduces to

$$
\bar{S}_m = \frac{2i(\rho_j/\rho_a) J_m(\sigma_s)}{(\pi\omega' r_0)(1-KM_s)} \; \frac{f_m(\eta_1) g_{m_\eta}(\eta_1) - g_m(\eta_1) f_{m_\eta}(\eta_1)}{[\,]_D} \tag{84}
$$

(Note that $M_s = M_j$ in this case of course.)

Additional Interfaces and "Matched" Solutions

Note that we have considered the shear layer to be linear, with uniform slope throughout. It is apparent that a more complex multi-slope profile, as sketched in Fig. 10a, could be studied by the same methods if conditions of continuous pressure and normal velocity are applied at each interface between linear segments of the shear-layer velocity profile (e.g. at $r = a$, $r = b$, in Fig. 10a). Each interface thus adds two equations to the set of simultaneous equations which must be solved for the transmission (and other) coefficients, and the form of the transmission coefficient is then somewhat more complicated than that shown in Eqs. (79) and (84).

Essentially the same method is employed when no single series-expansion of the shear layer solutions $f(\eta)$, $g(\eta)$ exists which is convergent over the entire shear layer (see paragraph following Eq. (55)). In this case the shear layer is divided by an imaginary interface at $r = r_e$, though the slope of the shear layer may be the same on either side of r_e (Fig. 10b). r_e is chosen anywhere in the region where both pairs of series-expansion formulas are valid; then one pair (Eqs. (48) and (49)) is useful in one part of the shear layer ($r_0 \leq r \leq r_e$) and the other pair (Eqs. (54) and (55)) is useful in $r_e \leq r \leq r_1$. Conditions of continuous pressure and continuous radial velocity at the imaginary interface $r = r_e$ add two equations to the set of simultaneous equations containing the unknown amplitude coefficients. Two forms of the transmission coefficient are obtained (for the single-slope velocity profile case) depending on whether the source radius r_s is greater or less than r_e. The solution is omitted here for brevity.

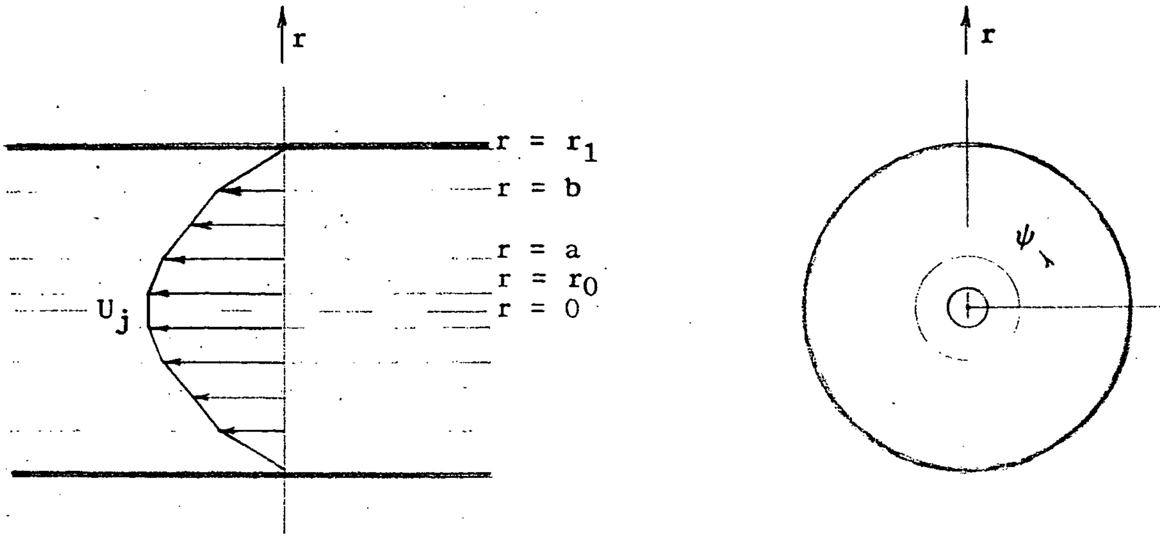

Fig. 10a JET WITH MULTI-SLOPE SHEAR LAYER.

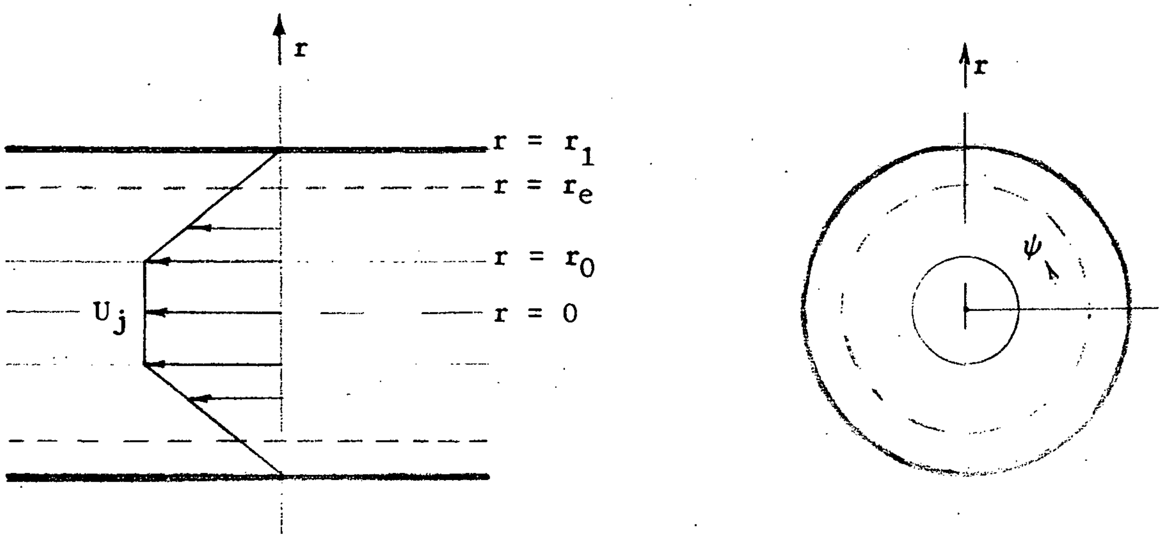

Fig. 10b SINGLE-SLOPE SHEAR-LAYER JET WITH IMAGINARY "INTERFACE" AT $r = r_e$.

Far-Field Result and Extension to Transient Source Case

The velocity potential outside the jet is

$$\phi_2 = \sum_0^{\infty} \int_{-\infty}^{\infty} \phi_{2_m}(K)\ dK \tag{85}$$

$\phi_{2m}(K)$, Eq. (67), contains the transmission coefficient $\overline{S}_m$, the determination of which has just been described. In the far field, the integral of Eq. (85) can be evaluated by the method of stationary phase. This analysis has previously been given in some detail for the two-dimensional jet case[2,3], and only the results for the circular cylindrical jet will be summarized here.

For $\sqrt{\alpha_T}\, M_s$ ($\equiv M_{a_s}$) < 1 there is only one point of stationary phase, located at $K = K_c$:

$$K_c = \sqrt{\alpha_T}\ (x/R^* - M_s\sqrt{\alpha_T})/(1-M_s{}^2\alpha_T) \tag{86}$$

where

$$R^* = \sqrt{x^2+(1-M_s{}^2\alpha_T)r^2} \equiv \sqrt{x^2+(1-M_{a_s}{}^2)r^2} \tag{87}$$

In the far field, then,

$$\phi_2 \rightarrow -2(\pi A/R^*) \sum_0^{\infty} \epsilon_m \cos\left[m(\psi-\psi_s)\right] \cdot$$

$$\cdot\ \text{R.P.}\left[i\ \overline{S}_m(K_c)\ e^{i(\omega'\gamma_c-\omega t-m\pi/2)}\right] \tag{88}$$

where

$$\omega'\gamma_c = \omega'\sqrt{\alpha_T}\left[R^* - M_s\sqrt{\alpha_T}x\right]/(1 - M_s{}^2\alpha_T) \tag{89}$$

Using $\overline{\Delta p^2} = \rho_a{}^2\ \overline{\phi_{2_t}{}^2}$ (with x = constant in taking the t derivative) gives the mean-square pressure in the far field:

$$\overline{\Delta p^2} \rightarrow \frac{2\pi^2 A^2 \rho_a{}^2 \omega^2}{R^{*2}(1-M_s{}^2\alpha_T)^2}\left[1 - \frac{\sqrt{\alpha_T}\, M_s x}{R^*}\right]^2 \sum_0^\infty \sum_0^\infty \epsilon_m \epsilon_n \cos\left[m(\psi-\psi_s)\right] \cdot$$

$$\cdot \cos\left[n(\psi-\psi_s)\right]\left[(S_m{}'S_n{}'+S_m{}''S_n{}'')\left[\cos(\tfrac{m\pi}{2})\cos(\tfrac{n\pi}{2})+\sin(\tfrac{m\pi}{2})\sin(\tfrac{n\pi}{2})\right]\right.$$

$$\left. + (S_m{}'S_n{}''-S_m{}''S_n{}')\left[\cos(\tfrac{m\pi}{2})\sin(\tfrac{n\pi}{2})-\sin(\tfrac{m\pi}{2})\cos(\tfrac{n\pi}{2})\right]\right] \qquad (90)$$

(n is used here and in Eq. (93) as a dummy index in the double summation.)

The analysis so far has been applied to the "permanent" source, i.e. an acoustical source drifting downstream with the local fluid for all time. For the sequence of transient sources described earlier $\overline{\Delta p^2}$ is obtained[3,4] by formally converting Eq. (90) to retarded coordinates and multiplying by $(1+M_{a_s}x_2/R)$. The retarded coordinates are $x_2, r, \psi; R$ where

$$R = \sqrt{x_2{}^2 + r^2}$$

The original coordinates fixed in the source are $x, r, \psi; R^*$ where R^* is defined by Eq. (87). The equations for coordinate transformation, from Refs. 3 or 4, are

$$\begin{aligned} R^* &= \left| R + M_{a_s} x_2 \right| \\ x &= x_2 + M_{a_s} R \end{aligned} \qquad (91)$$

Changing to retarded coordinates the critical K values become

$$K_c = \sqrt{\alpha_T}\,(x_2/R)/(1+\sqrt{\alpha_T}\,M_s x_2/R) \qquad (92)$$

or, in the notation of Eq. (64),

$$K_{a_c} = (x_2/R)/(1+M_{a_s}x_2/R) \qquad (92a)$$

$\overline{\Delta p^2}$ for the transient source sequence is

$$\overline{\Delta p^2(\psi_s)} = \frac{2\pi^2 A^2 \rho_a{}^2 \omega^2}{R^2 \left|1+M_{a_s} x_2/R\right|^3} \sum_0^\infty \sum_0^\infty \epsilon_m \epsilon_n \cos\left[m(\psi-\psi_s)\right] \cos\left[n(\psi-\psi_s)\right] \cdot$$

$$\cdot \left[(S_m{}' S_n{}' + S_m{}'' S_n{}'') \left[\cos(\tfrac{m\pi}{2})\cos(\tfrac{n\pi}{2}) + \sin(\tfrac{m\pi}{2})\sin(\tfrac{n\pi}{2})\right] \right.$$

$$\left. + (S_m{}' S_n{}'' - S_m{}'' S_n{}') \left[\cos(\tfrac{m\pi}{2})\sin(\tfrac{n\pi}{2}) - \sin(\tfrac{m\pi}{2})\cos(\tfrac{n\pi}{2})\right] \right] \tag{93}$$

Note that each transient source is assumed to go through many cycles. The transmission coefficients are evaluated at K_c (Eq. (92)). When the absolute magnitude of the $\left|1+M_{a_s} x_2/R\right|$ factor is used, as indicated, Eq. (93) is applicable for $M_{a_s} \gtrless 1$.

Eq. (93) is the far-field mean-square pressure for <u>one</u> source (i.e. one transient source sequence) located at $\psi = \psi_s$, $r = r_s$. Since the jet is symmetrical we can expect, on the average, to find a similar source located at any ψ_s around the jet, each with random phase relative to all of the others. Their mean-square pressures are additive. The <u>average</u> mean-square pressure due to a ring of random-phase sources is

$$\overline{\Delta p^2} = \frac{1}{2\pi} \int_0^{2\pi} \overline{\Delta p^2(\psi_s)}\, d\psi_s \tag{94}$$

or

$$\frac{\overline{\Delta p^2}\, R^2}{2\pi^2 A^2 \rho_a{}^2 \omega^2} = \frac{1}{\left|1+M_{a_s} x_2/R\right|^3} \sum_0^\infty \epsilon_m (S_m{}'^2 + S_m{}''^2) \tag{95}$$

Note that each value of m in Eq. (95) represents the average mean-square pressure in the far field due to a transient ring-source having source strength proportional to $\cos\left[m(\psi - \psi_S)\right]$. Since each of the ring sources with $m > 0$ has zero net source strength, it might be expected that radiation from positive sections of the ring would tend more and more to cancel the radiation from negative sections of the ring, so the net acoustic radiation into the far field would be small for large m. Computations for subsonic jet examples indicate this to be the case (though it may not be true for supersonic jets). When $M_j < 1$ the terms of Eq. (95) tend to drop rather quickly in magnitude as m increases from zero, so that in practice only a few terms in the summation usually are required, and computing time is thereby benefited.

B. RESULTS FOR JET TEMPERATURE = AMBIENT TEMPERATURE

This section contains a comparison of far-field mean-square pressures produced by sources in circular cylindrical jets and in two-dimensional jets, at subsonic velocities. Comparisons are made for the following conditions:

1. Source at the center of a high Mach number subsonic jet.
2. Source in the shear layer of a high Mach number subsonic jet.
3. Source in an extended constant-velocity region centrally located in a high Mach number subsonic

jet.

4. Source at the center of a low Mach number jet.

For the two-dimensional jet, pressures were evaluated only in streamwise planes containing the source and normal to the plane of the jet. A simulation of circular jet effects from such data would at least require evaluation of pressures in planes other than normal to the two-dimensional jet plane. Some of the differences between circular and two-dimensional jet effects pointed out in the following pages can in a crude sense be attributed to the neglect of non-normal planes in the two-dimensional calculations.

1. Source at the Center of the Jet; $M_j = 0.7$

In Fig. 11 the far-field mean-square pressures are shown for a source at the center of a circular cylindrical jet. The maximum Mach number in the jet is 0.7 which is held constant throughout a small region near the jet center. The radius of this region is 0.1 times the jet radius, and the jet velocity varies linearly outside this region to a value of zero at the edge of the jet. The numerical calculations are simplified by having a central constant-velocity region, and the cross-sectional area of the central region is in this case only one-percent of the total cross-sectional area of the jet. Strouhal numbers (S_T) of 0.1, 0.2, 0.5 and 1.0 are shown, where

$$S_T = \frac{\omega}{2\pi} \frac{\text{(jet diameter)}}{\text{(maximum jet velocity)}} .$$

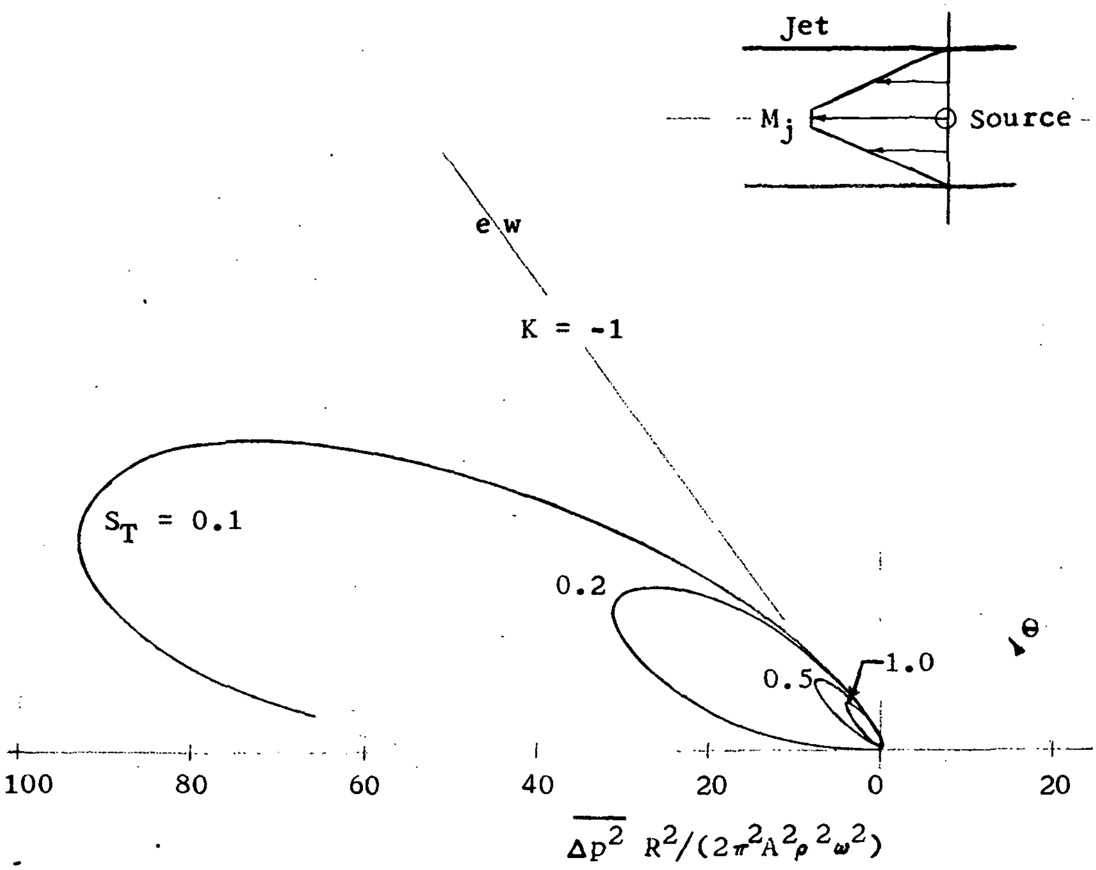

Fig. 11 FAR-FIELD MEAN-SQUARE PRESSURE DUE TO A SOURCE AT THE CENTER OF A CIRCULAR JET. $M_j = 0.7$; $\bar{r}_0 = 0.1$.

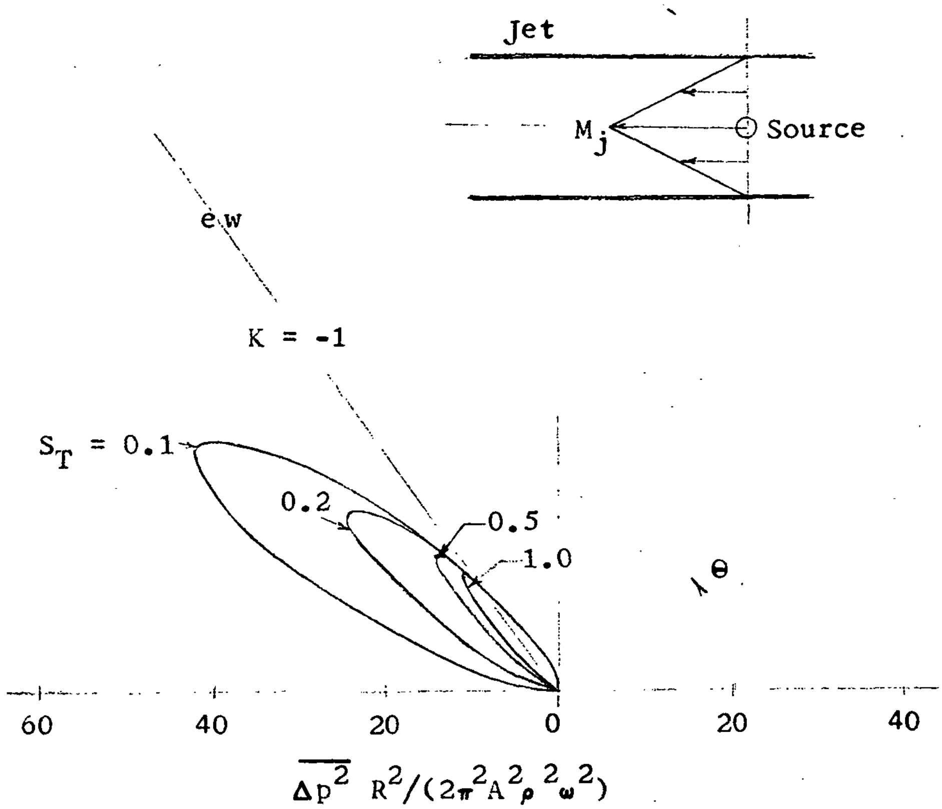

Fig. 12 FAR-FIELD MEAN-SQUARE PRESSURE DUE TO A SOURCE AT THE CENTER OF A TWO-DIMENSIONAL JET. $M_j = 0.7$; $\overline{z}_0 = 0$.

For comparison Fig. 12 shows far-field mean-square pressures for a source at the center of a two-dimensional jet. Again the maximum Mach number of the jet is 0.7. The jet velocity varies linearly from the jet center to the edge, although for strict comparison one should perhaps maintain a central constant-velocity region with thickness one-percent of the jet thickness.

Comparison of Figs. 11 and 12 shows that for the circular cylindrical jet the pressure lobes are wider and are rotated in closer to the downstream axis. For a Strouhal number of 0.2 the mean-square pressures are of similar magnitude. However the variation of mean-square pressure with Strouhal number is considerably greater for the circular jet.

On Figs. 11 and 12 (and most following figures) the radial line with e on one side and w on the other indicates the boundary between the region in which the disturbances leaving the source might be termed "pseudo-sound" (e) and are exponentially decaying in z (or r) and the region in which disturbances leaving the source are "true sound", or true waves (w). It is evident that most of the far-field noise for the examples shown in Figs. 11 and 12 is produced by disturbances originating as pseudo-sound.

All of the pressure lobes obtained in this study are closed curves, i.e. $\overline{\Delta p^2} \rightarrow 0$ as $\theta \rightarrow 0$ and as $\theta \rightarrow \pi$. The plotted curves have sometimes not been completed in the vicinity of $\theta = \pi$ (as, for example, the $S_T = 0.1$ curve in Fig. 11). This is because the computer output was obtained only for certain specified θ-values which in some cases were not closely enough spaced to allow good fairing of the $\overline{\Delta p^2}$-curves near $\theta = \pi$. This is a small region, however, and we have simply left that part of the curves unplotted, since it did not seem worthwhile to re-run the program with more θ-values.

2. Source in the Shear Layer

Fig. 13 shows far-field mean-square pressures for a source half-way out in the shear layer of a circular cylindrical jet. The source therefore travels at half the maximum jet velocity and its Mach number is 0.35, while the small constant-velocity region at the center of the jet has a Mach number of 0.7. Comparing this with Fig. 14, a corresponding case for the two-dimensional jet, we see again that the pressure lobes are broadened and extend in closer to the downstream axis. For the lower Strouhal numbers the variation of mean-square pressure with Strouhal number is increased as before. For $S_T = 1$ and $S_T = 2$ the two-dimensional jet shows a reversal in trend with the peaks moving out from the downstream axis. This reversal does not appear for the circular jet, though it might occur at still higher S_T values. Such effects might appear as the wavelength of the sound is reduced to the order of the jet diameter. For the smaller Strouhal numbers, the far-field noise again mainly originates at the source as pseudo-sound, but this is less true as the Strouhal number increases.

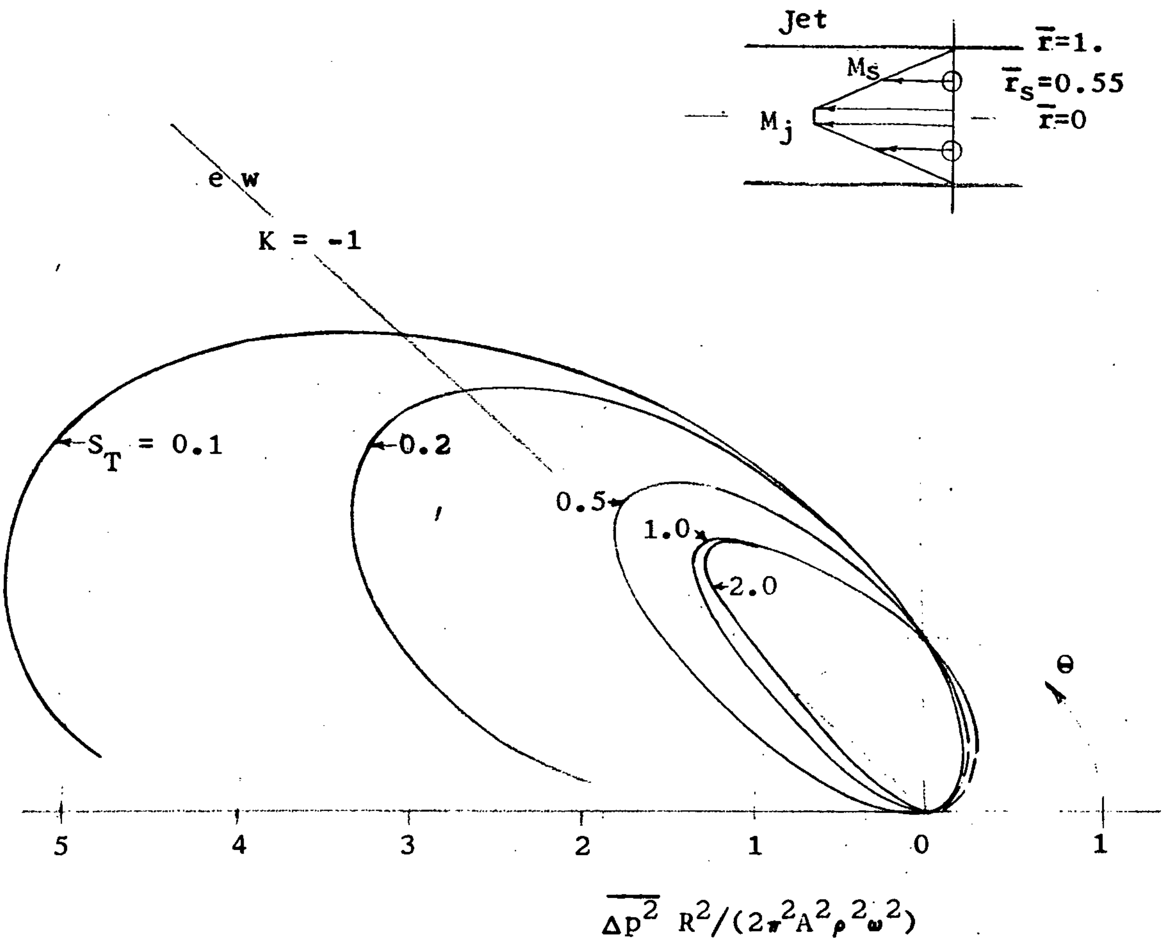

Fig. 13 FAR-FIELD MEAN-SQUARE PRESSURE DUE TO A SOURCE HALF-WAY OUT IN THE SHEAR LAYER OF A CIRCULAR JET. $M_j = 0.7$; $M_s = 0.35$; $\bar{r}_0 = 0.1$

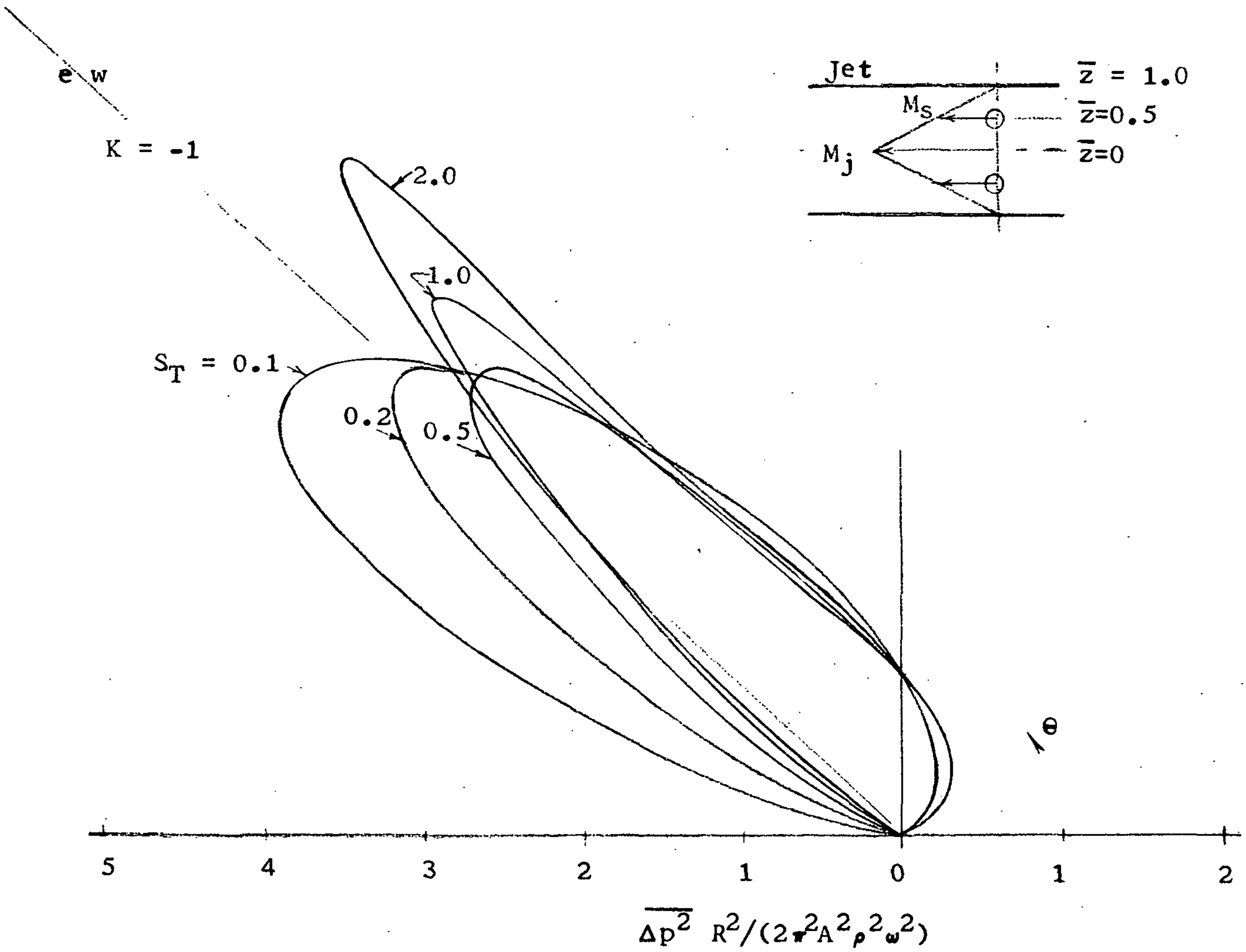

Fig. 14 FAR-FIELD MEAN-SQUARE PRESSURE DUE TO A SOURCE HALF-WAY OUT IN THE SHEAR LAYER OF A TWO-DIMENSIONAL JET. $M_j = 0.7$; $M_s = 0.35$; $\bar{z}_0 = 0$.

3. Source in an Extended Constant-Velocity Region Centrally Located in a High-Velocity Jet

For the example chosen the constant-velocity region in the circular jet extends from the center to one-half the total jet radius, and in the two-dimensional jet from the center to one-quarter of the jet semi-thickness. In each case one-quarter of the cross-sectional area of the jet is in the constant-velocity region.

In Figs. 15 and 16 mean-square pressures (in the far field) are shown for sources at the center and at the edges of the constant-velocity region. The maximum jet Mach number is 0.7 and the Strouhal number is 0.2 in all cases. For the circular jet (Fig. 15) a source at the center produces slightly lower pressures than sources at the edge of the constant-velocity region. This occurs in the angular range where source disturbances decay exponentially in the central region (angles (θ) greater than 126-degrees), and it is probably this exponential decay which weakens the effect of the source at the center. The two-dimensional jet, Fig. 16, shows a similar result, the effectiveness of the sources progressively decreasing as their disturbances have to traverse increasing thicknesses of the central region.

The pressure lobes for the circular jet are somewhat broader and rotated in slightly towards the downstream axis by comparison with the two-dimensional jet. At this one Strouhal number of 0.2 the pressures are appreciably lower for the circular jet.

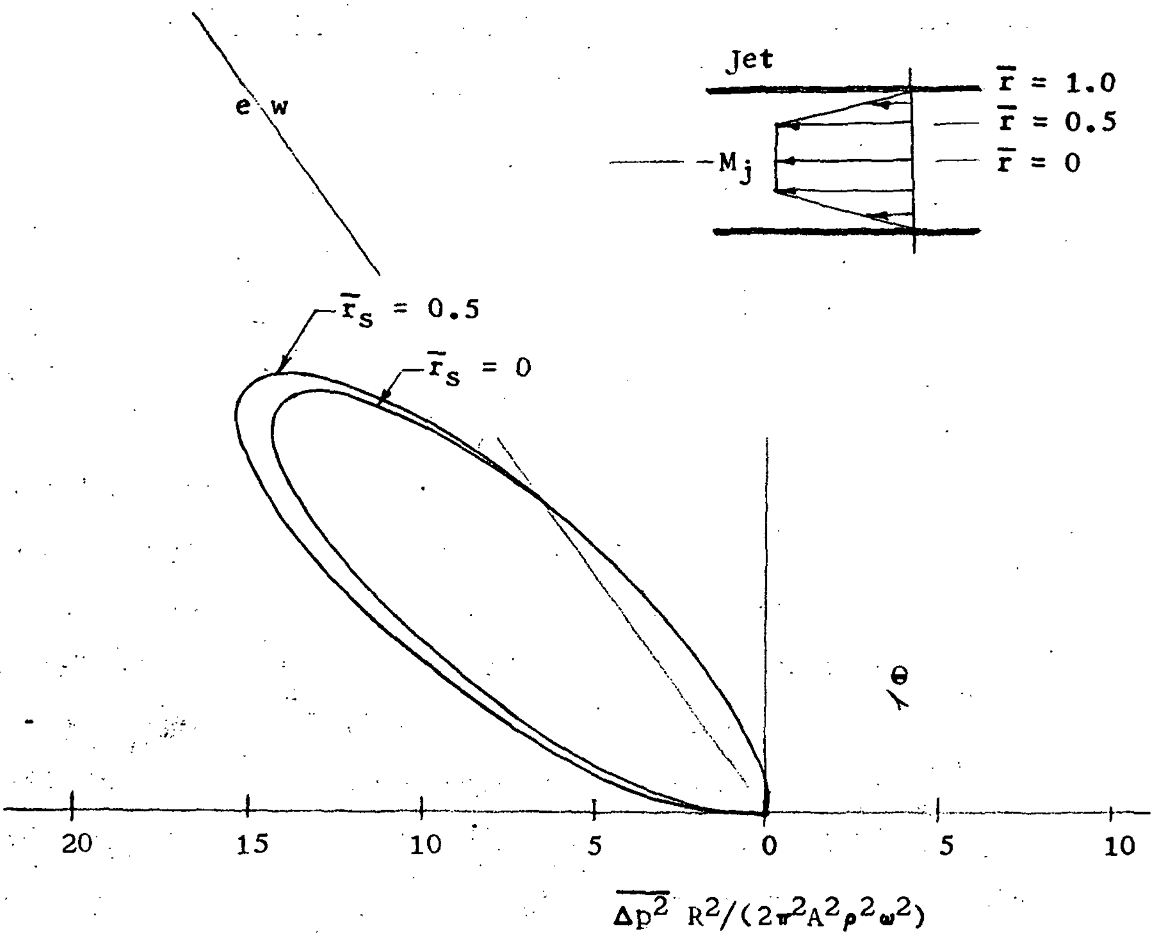

Fig. 15 MEAN-SQUARE PRESSURE IN THE FAR FIELD DUE TO A SOURCE IN A CIRCULAR JET, FOR TWO SOURCE LOCATIONS: $\bar{r}_s = 0$ and $\bar{r}_s = 0.5$. $M_j = 0.7$; $S_T = 0.2$; $\bar{r}_0 = 0.5$.

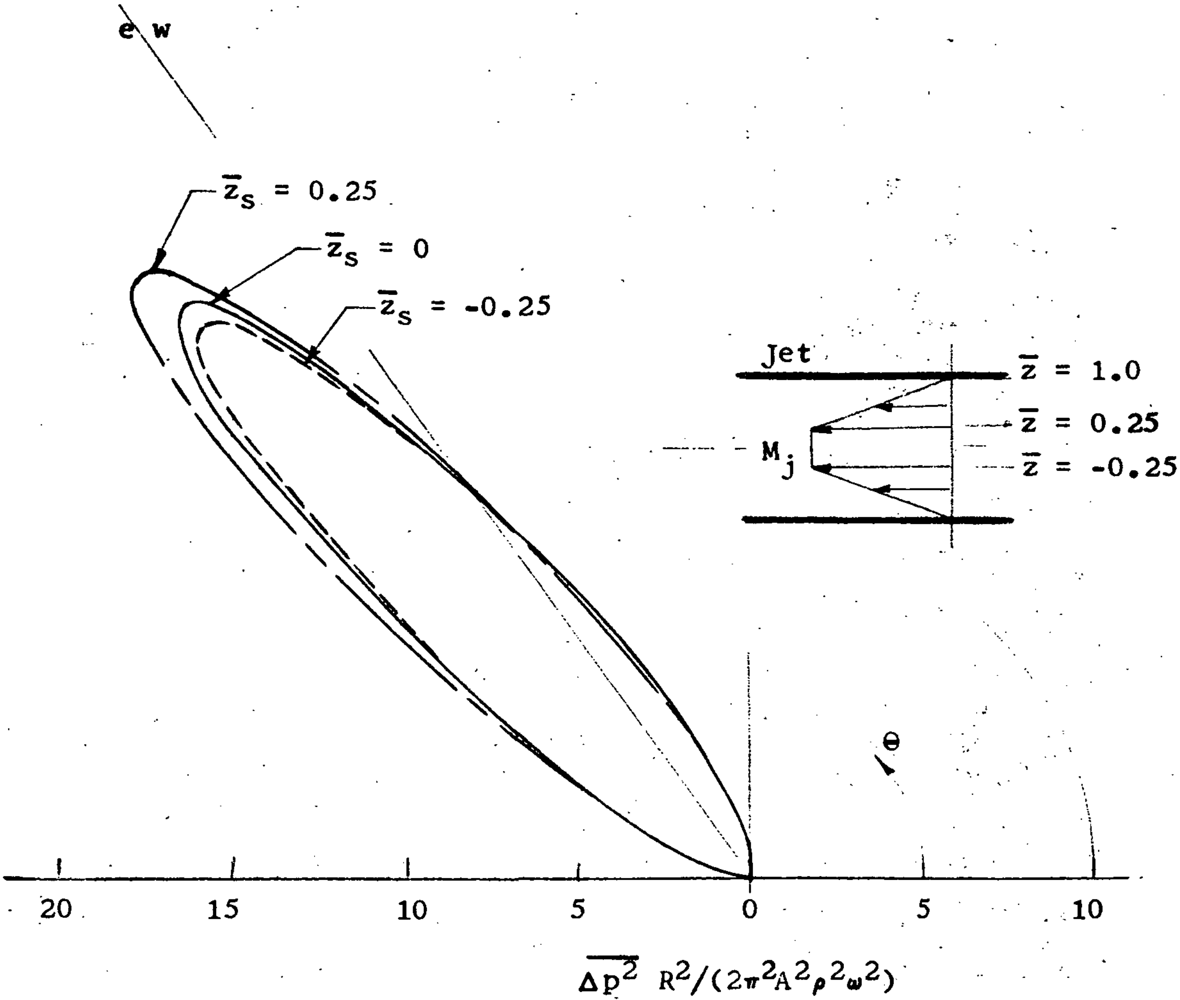

Fig. 16 MEAN-SQUARE PRESSURE IN THE FAR FIELD DUE TO A SOURCE IN A TWO-DIMENSIONAL JET, FOR THREE SOURCE LOCATIONS: $\bar{z}_s = 0$ (center of jet), $\bar{z}_s = 0.25$ (nearer edge of central constant-velocity region) and $\bar{z}_s = -0.25$ (farther edge of central region). $M_j = 0.7$; $S_T = 0.2$; $\bar{z}_0 = 0.25$.

4. Source at the Center of a Low Mach Number Jet

Figs. 17 and 18 show far-field mean-square pressures for sources at the center of a Mach 0.3 jet. In the two-dimensional jet (Fig. 18) the velocity falls off linearly from the center to the outer edge. In the circular jet (Fig. 17) the velocity is constant out to 0.1 times the jet radius, and then falls off linearly to the outer edge. (Only one-percent of the jet cross-sectional area is in this central region.)

As in the higher Mach number case, the principle effects of changing from the two-dimensional to the circular jet are, first, that the pressure lobes broaden and extend in closer to the downstream axis and, second, that the pressure variation with Strouhal number is accentuated.

Note again the radial line marking the boundary between the region where disturbances leaving the source are pseudo-sound (e) and the region where disturbances leaving the source are true waves (w). At a Mach number of zero (a trivial case not shown here, with $\overline{\Delta p^2}\ R^2/(2\pi^2 A^2 \rho^2 \omega^2) = 1$) all far-field noise is produced by disturbances which leave the source as true sound. It is therefore remarkable that at a Mach number of only 0.3 most of the far-field noise is produced by disturbances originating as pseudo-sound. Since pseudo-sound corresponds to the 90-degree out-of-phase components of pressure and velocity it transmits energy only by interference with reflected waves. In the transmission through the jet these exponentially decaying disturbances become true waves, and so can transmit energy to the far field without assistance.

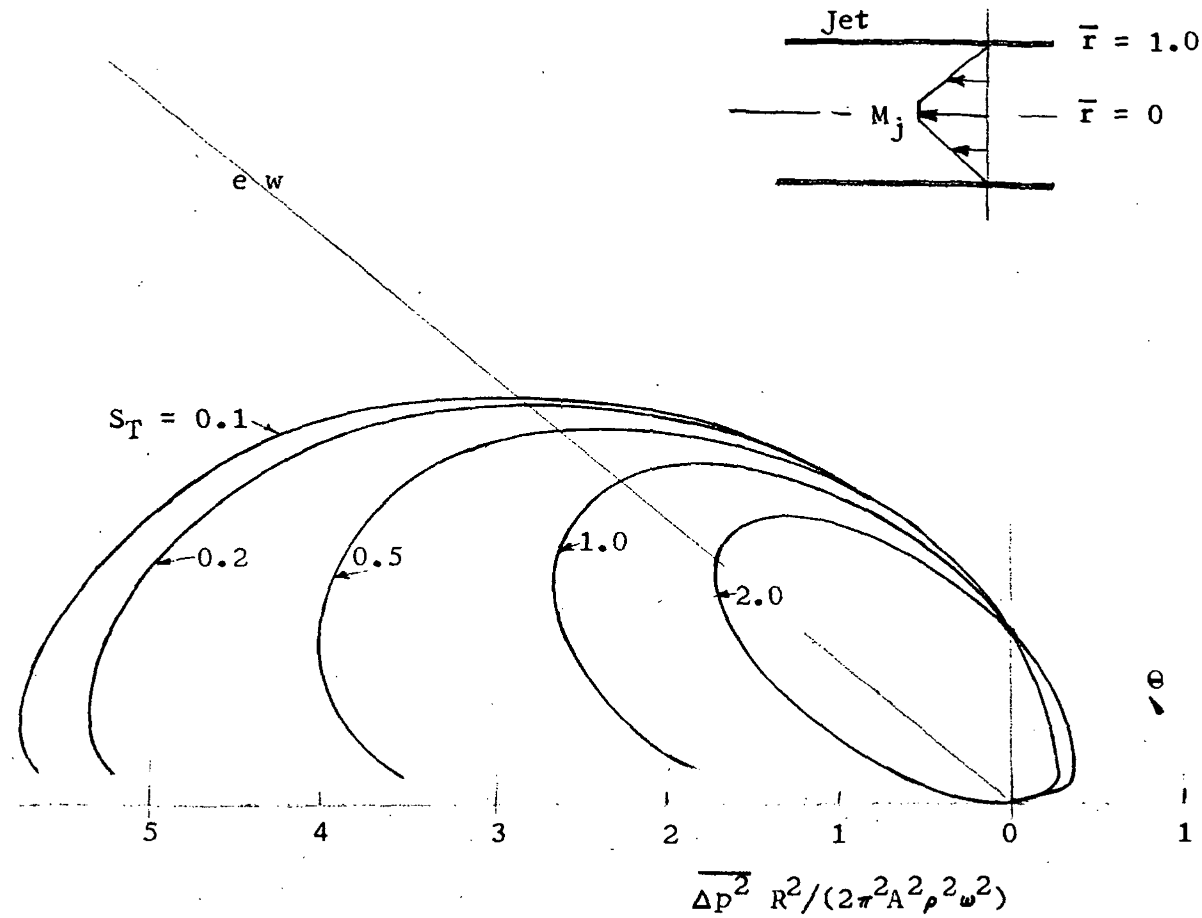

Fig. 17 FAR-FIELD MEAN-SQUARE PRESSURE DUE TO A SOURCE AT THE CENTER OF A CIRCULAR JET

$M_j = 0.3$; $\bar{r}_0 = 0.1$

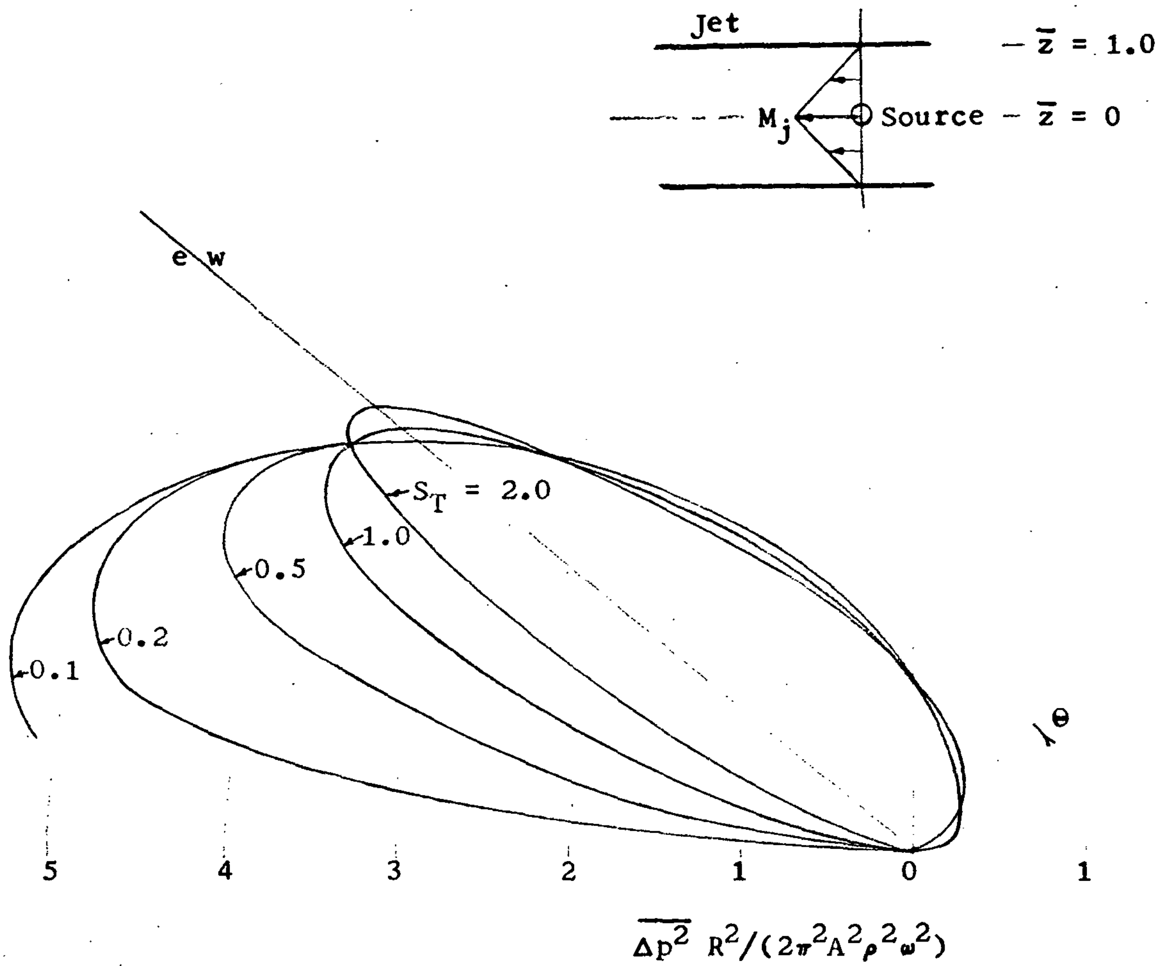

Fig. 18 FAR-FIELD MEAN-SQUARE PRESSURE DUE TO A SOURCE AT THE CENTER OF A TWO-DIMENSIONAL JET. $M_j = 0.3$; $\bar{z}_0 = 0$.

C. RESULTS FOR JET TEMPERATURE ABOVE AMBIENT TEMPERATURE

As an example for numerical computations, we have chosen a circular cylindrical jet with uniform velocity throughout a core covering the inner half of the total radius. The velocity decreases linearly over the outer half radius, reaching zero at the outer edge of the jet. All comparisons are made at fixed jet velocity, so that the jet Mach number based on the ambient speed of sound is 0.7 ($M_{aj} = 0.7$). (Qualitatively similar results, not shown here, are obtained at a Mach number of 0.3.) The ratio of jet temperature (uniform across the jet) to ambient temperature is designated by α_T, and values of 1, 2, 4 and 6 are considered.

Figs. 19 - 22 show results for Strouhal numbers of 0.2, 0.1, 0.01, and 0.001, respectively. The very low Strouhal numbers are included to show that in the limit of zero frequency (or zero jet diameter) the temperature effect disappears. The curves then merge and the value of $\overline{\Delta p^2} R^2/(2\pi^2 A^2 \rho_a{}^2 \omega^2)$ becomes $|1+M\cos\theta|^{-5}$, which is the value for a modified moving source[5]. At higher Strouhal numbers (up to and including 0.2, at least) increasing the jet temperature reduces the magnitude of the pressure lobes and rotates them away from the downstream jet axis. This trend may alter at still higher Strouhal numbers, which have not yet been investigated.

It must be remembered that the source strength here is $8\pi^2 A$, and represents the maximum volume introduced by the pulsating source per unit time. Only if this source strength is unaffected by heating the jet (with velocity profile fixed) will the reduction in mean-square pressure with increasing jet temperature be observed.

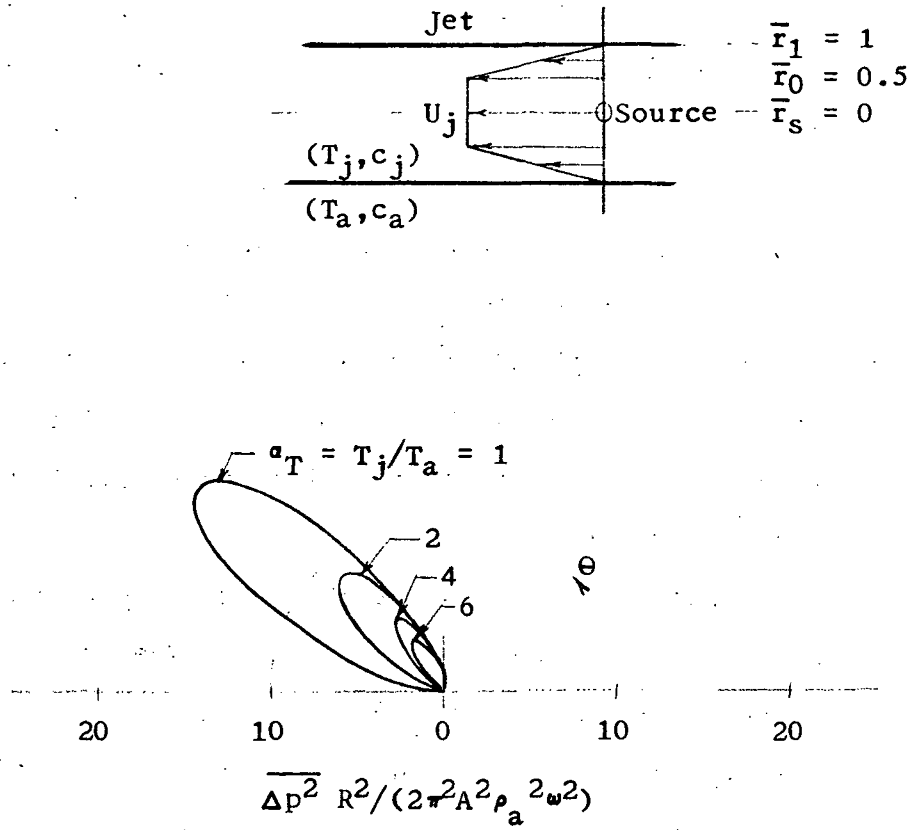

Fig. 19 FAR-FIELD MEAN-SQUARE PRESSURE DUE TO SOURCE AT CENTER OF UNIFORMLY HEATED CIRCULAR JET. $M_{aj} = U_j/c_a = 0.7$; $S_T = 0.2$; $\bar{r}_0 = 0.5$.

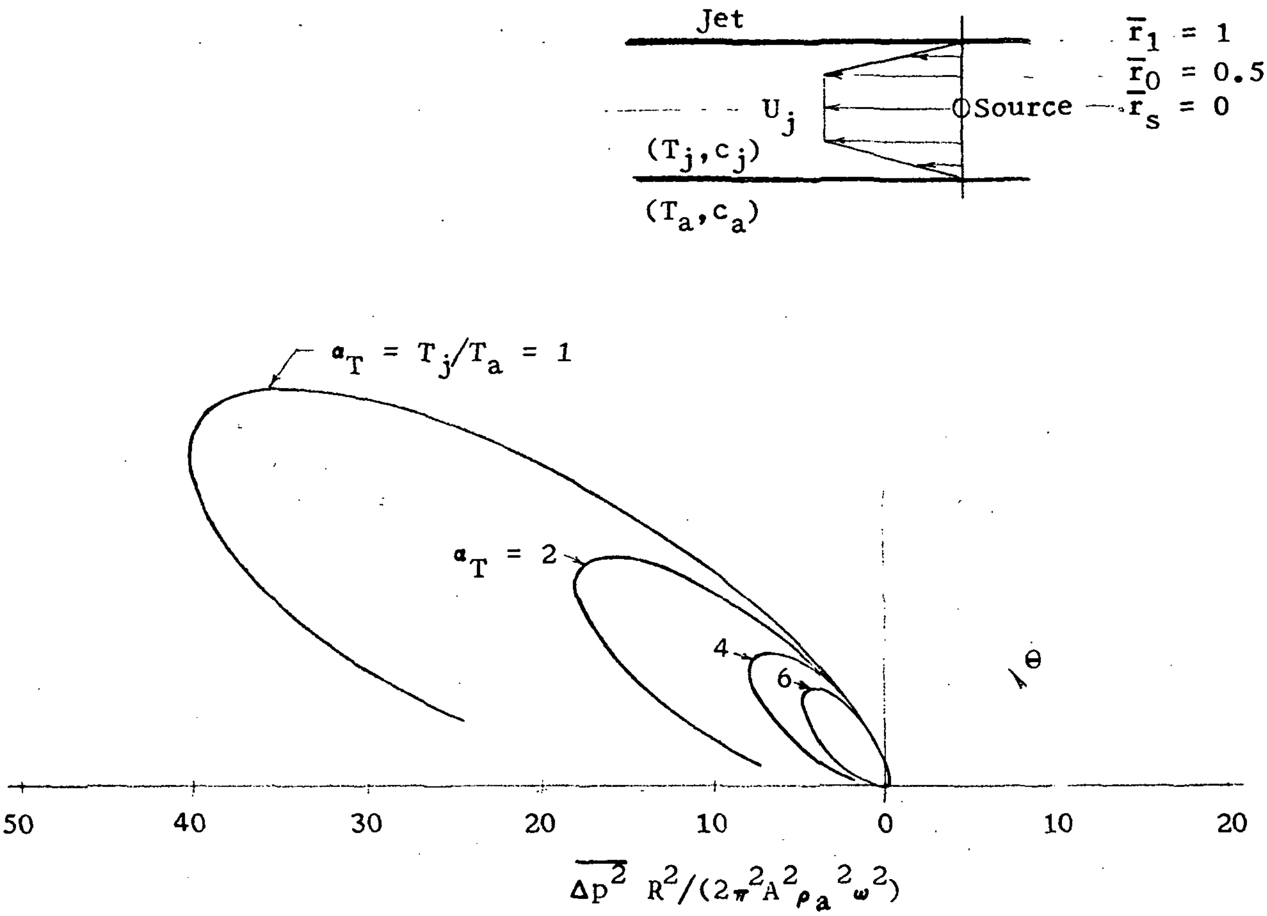

Fig. 20 FAR-FIELD MEAN-SQUARE PRESSURE DUE TO SOURCE AT CENTER OF UNIFORMLY HEATED CIRCULAR JET. $M_{aj} = U_j/c_a = 0.7$; $S_T = 0.1$; $\bar{r}_0 = 0.5$.

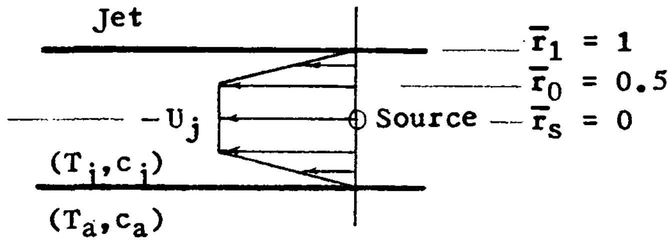

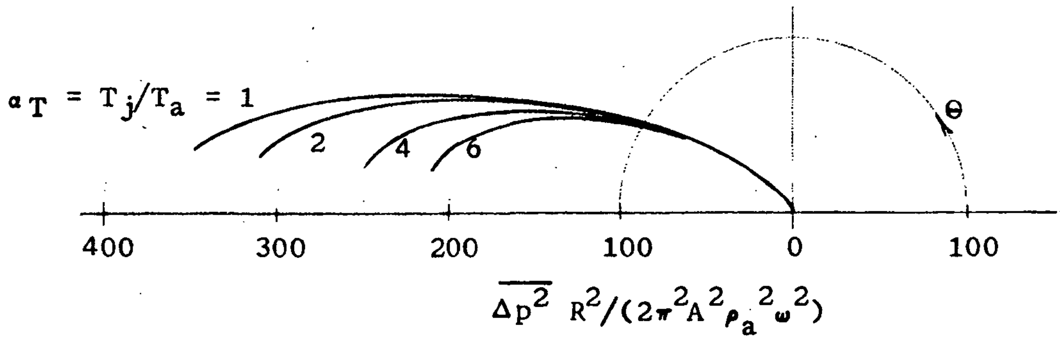

Fig. 21 $M_{aj} = U_j/c_a = 0.7$; $S_T = 0.01$; $\bar{r}_0 = 0.5$.

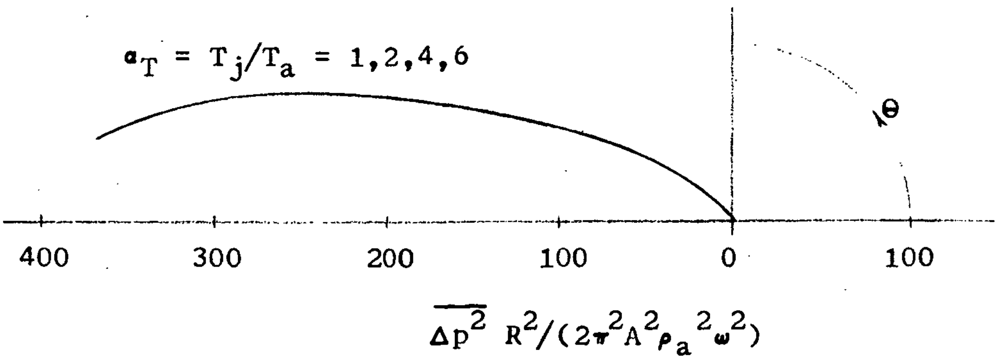

Fig. 22 $M_{aj} = U_j/c_a = 0.7$; $S_T = 0.001$; $\bar{r}_0 = 0.5$.

FAR-FIELD MEAN-SQUARE PRESSURE DUE TO SOURCE AT CENTER OF UNIFORMLY HEATED CIRCULAR JET.

6. PRELIMINARY ANALYSIS FOR LINEARLY VARYING TEMPERATURE IN JETS

Introduction

In previous analyses we have considered mean* velocity variations across the jet, but the mean temperature of the jet has been held constant (either at the ambient value or higher). Here we permit temperature to vary across the jet also, and carry the development as far as the ordinary differential equation for the shear layer in both two-dimensional and circular jets.

For simplicity we show the development only for the two-dimensional jet. The ordinary differential equation for pressure as a function of z has one singular point if the temperature is constant. This singular point may be in the region of interest (the shear layer) or outside it. In the former case the expansion must be made about this point and is everywhere convergent. Linearly varying temperature introduces a second singular point where $T = 0$. This point never falls in the region of interest, but it does limit the radius of convergence for the expansion about any other point. In some cases two matched expansions are then required, which complicates the computation.

In a circular jet a third singular point appears (at the center of the jet) and this, imposing further limits on convergence, might require more than two matched expansions in some cases. Thus the programming of the calculations would be more complicated for the circular jet.

---

*mean refers to a time average eliminating turbulent velocities.

Development of Equations for Two-Dimensional Jet

Let x,y,z be coordinates measured longitudinally, laterally and normal to the "plane" of the two-dimensional jet, and u,v,w be the corresponding velocities. Then, indicating perturbation quantities (which are functions of x,y,z and t) by Δu, etc., we have

$$
\begin{aligned}
u &= U(z) + \Delta u \\
v &= \Delta v \\
w &= \Delta w \\
T &= T_o(z) + \Delta T \\
\rho &= \rho_o(z) + \Delta\rho \\
p &= p_o + \Delta p
\end{aligned}
$$

where

$$p_o = \text{constant} = p_{ambient} = \rho_o(z)\, R\, T_o(z)$$

and where R is the gas constant, assumed fixed. U(z) gives the mean velocity profile, $T_o(z)$ the mean temperature profile and $\rho_o(z)$ the mean density profile. The mean pressure, p_o, is constant throughout the jet and ambient fluid, and the mean temperature and density profiles are simply related through the equation of state. The dynamical equations can now be written as[8]

$$
\begin{aligned}
&\Delta u_t + U(z)\,\Delta u_x + \Delta w\, U_z(z) + \frac{\Delta p_x}{\rho_o(z)} = 0 \\
&\Delta v_t + U(z)\,\Delta v_x + \frac{\Delta p_y}{\rho_o(z)} = 0 \qquad (96) \\
&\Delta w_t + U(z)\,\Delta w_x + \frac{\Delta p_z}{\rho_o(z)} = 0
\end{aligned}
$$

and the equation of continuity becomes

$$\Delta\rho_t + U(z)\,\Delta\rho_x + \rho_o(z)\left[\Delta u_x + \Delta v_y + \Delta w_z\right] + \rho_{o_z}\,\Delta w = 0 \qquad (97)$$

Here we have four equations and five unknowns: Δu, Δv, Δw, Δp and $\Delta\rho$. However, if we assume that the entropy of each fluid element is unchanged when an acoustic wave passes through (e.g. see Blokhintsev[10], NACA TM 1399, p. 21) then, following a fluid particle,

$$\frac{d(\Delta p)}{d(\Delta\rho)} = k(z)\,\gamma\left[\rho_o(z)\right]^{\gamma-1} = \gamma R T_o(z) = c^2(z) \qquad (98)$$

where $k(z)$ is the adiabatic constant for a given z and γ is the ratio of specific heats. (Note that entropy is not assumed constant throughout the jet nor even at one point in the jet.) $c(z)$ is the local speed of sound.

From Eq. (98)

$$\frac{d\Delta\rho}{dt} = \frac{d\Delta p}{dt}\,\frac{1}{c^2(z)} \qquad (99)$$

Also, the substantial derivatives, $d\Delta\rho/dt$ and $d\Delta p/dt$, are

$$\begin{aligned}\frac{d\Delta\rho}{dt} &= \Delta\rho_t + \rho_{o_z}(z)\,\Delta w + U(z)\,\Delta\rho_x \\ \frac{d\Delta p}{dt} &= \Delta p_t + U(z)\,\Delta p_x\end{aligned} \qquad (100)$$

Eliminating $d\Delta\rho/dt$ and $d\Delta p/dt$ between Eqs. (99) and (100):

$$\Delta\rho_t + U(z)\,\Delta\rho_x = \frac{1}{c^2(z)}\left[\Delta p_t + U(z)\,\Delta p_x\right] - \rho_{o_z}(z)\,\Delta w \qquad (101)$$

This relation between Δp and $\Delta\rho$ gives us the required added equation to make the previous set determinate. If, for convenience, we express Δp as

$$\Delta p = \rho_o(z)\ c^2(z)\ \sigma \tag{102}$$

(noting that $\rho_o(z)\ c^2(z)$ is a constant), then the four equations become

$$\begin{aligned}
&\Delta u_t + U(z)\,\Delta u_x + U_z(z)\,\Delta w + c^2(z)\,\sigma_x = 0 \\
&\Delta v_t + U(z)\,\Delta v_x + c^2(z)\,\sigma_y = 0 \\
&\Delta w_t + U(z)\,\Delta w_x + c^2(z)\,\sigma_z = 0 \\
&\sigma_t + U(z)\,\sigma_x + \Delta u_x + \Delta v_y + \Delta w_z = 0
\end{aligned} \tag{103}$$

Eliminating Δu, Δv and Δw gives

$$\begin{aligned}
&\sigma_{ttt} + 3\,U(z)\,\sigma_{ttx} + 3\,U^2(z)\,\sigma_{txx} + U^3(z)\,\sigma_{xxx} \\
&\quad - c^2(z)\left[(\nabla^2\sigma)_t + U(z)\,(\nabla^2\sigma)_x\right] + 2\,U_z(z)\,c^2(z)\,\sigma_{zx} \\
&\quad - \left[c^2(z)\right]_z\left[\sigma_{zt} + U(z)\,\sigma_{zx}\right] = 0
\end{aligned} \tag{104}$$

For $\left[c^2(z)\right]_z = 0$ (i.e. a constant temperature jet) σ becomes s, the condensation, and Eq. (104) becomes Eq. 3 of Ref. 4 or Eq. 5 of Ref. 1.

For $U(z) \equiv 0$, the case of a static heated layer, we get

$$\nabla^2\sigma = \frac{1}{c^2(z)}\left[\sigma_{tt} - \left[c^2(z)\right]_z\,\sigma_z\right] \tag{105}$$

Returning to Eq. (104), let

$$\sigma(x,y,z,t) = F(z)\cos(k_2 y)\sin(k_1 x - \omega t)$$

Substituting this in Eq. (104) gives an ordinary differential equation for F as a function of z.

$$F_{zz} + F_z\left[\frac{2U_z k_1}{(\omega - Uk_1)} + \frac{(c^2)_z}{c^2}\right] + F\left[\frac{(\omega - Uk_1)^2}{c^2} - k^2\right] = 0 \qquad (106)$$

The simplest temperature (or c^2) variation with z is linear. In that case the equation has two singular points: one, where $(\omega - Uk_1) = 0$, may fall within the region of interest (the linear shear layer); the other, where $c^2 = 0$, never lies in the region of interest. If F is expanded as a power series in z, one expansion must be made about each singular point in the region of interest. Other singular points limit the radius of convergence of such expansions and may require the use of matched expansions about two different points. Such procedures have already been described in connection with the circular jet at constant temperature, which has two singular points.

The Circular Cylindrical Jet

For the circular cylindrical jet the axial, angular and radial coordinates are x, ψ and r. The corresponding perturbation velocities are u,v,w.

The partial differential equation for σ is

$$\sigma_{ttt} + 3\,U\,\sigma_{ttx} + 3\,U^2\,\sigma_{txx} + U^3\,\sigma_{xxx}$$

$$- c^2\left[(\nabla^2\sigma)_t + U\,(\nabla^2\sigma)_x\right] + 2\,U_r\,c^2\,\sigma_{rx}$$

$$- (c^2)_r\left[\sigma_{rt} + U\,\sigma_{rx}\right] = 0 \qquad (107)$$

where $U = U(r)$, $c^2 = c^2(r)$ and the perturbation pressure, Δp, is $\Delta p = \rho_o(r)\,c^2(r)\,\sigma$. ($\rho_o(r)\,c^2(r)$ is a constant).

If we let

$$\sigma(x,\psi,r,t) = F(r)\,\cos(m\psi)\,\sin(kx-\omega t)$$

then $F(r)$ is defined by

$$F_{rr} + F_r\left[\frac{2U_r k}{(\omega-Uk)} + \frac{1}{rc^2}\,\frac{d(rc^2)}{dr}\right] + F\left[\frac{(\omega-Uk)^2}{c^2} - \left(k^2 + \frac{m^2}{r^2}\right)\right] = 0 \qquad (108)$$

Note that k here corresponds to k_1 in the two-dimensional jet.

For temperature (or c^2) varying linearly with r, singular points occur for $(\omega-Uk) = 0$, $r = 0$ and $c^2 = 0$. Obtaining solutions by series expansions is therefore more complicated than in the two-dimensional case which has only two singular points instead of three.

7. DISCUSSION OF APPLICABILITY

As stated earlier this work is not intended to provide a comprehensive theory of the noise produced by turbulence in jets. Instead, we have concentrated on one aspect of the problem with the purpose of providing facts (not intuitively evident) which can be used in formulating a more comprehensive theory. Utilization of this material in a more general theory requires consideration of a number of factors. Some of these (not necessarily in order of importance) are as follows:

(1) What singularity (source, dipole, quadrupole or other type) should be considered as the noise generator?

(2) Since we consider that turbulence is the only true generator, we are interested in experimental methods capable of distinguishing between turbulent velocity fluctuations (associated with vorticity and non-linear terms) and the linear fluctuations associated with transmission in our analysis.

(3) Frequencies recorded by an instrument at rest in the ambient fluid are not the same as the generating frequencies (because of the Doppler effect). The frequency correction is easily made, but the plotting of mean-square pressure curves for fixed observed frequencies requires the use of an energy spectrum, since a given generating frequency produces different observed frequencies at different angular positions in the far field.

(4) Various generating regions of the jet must be considered.

(5) The limitations imposed by considering the jet to be infinitely long should be studied, especially at low frequencies.

The final factor ((5)) is now considered in some detail. There are really two parts to this question. The first part might be stated as follows: Assuming coordinates fixed in the source, how much of the jet upstream and downstream of the source is really essential to the analysis? The second part of the question relates to the transient source analysis in retarded coordinates: How far does a given transient source travel relative to the nozzle, and can it be assumed to pass through many cycles in this lifetime?

The first part of the question relates to refraction effects, which do not appear explicitly in Lighthill's work. However, the second part of the question relates to convection effects and so may apply also to Lighthill's analysis.

Part 1 (coordinates fixed in the source)

When the generating frequency is low the wavelength of the disturbance is large, and may be many times the jet thickness. Our analysis deals primarily with wavelengths in the streamwise direction and, since we assume an infinitely long jet, many cycles may appear in the jet for any given wavelength. On the other hand, in a real jet of finite length, perhaps only a fraction of a cycle may appear. This raises a question as to the applicability of our analysis at low frequency.

However, in certain cases we have examined the results obtained for infinitely long jets in the limit of zero frequency. For example[5] a source drifting with the fluid in an infinitely long jet becomes a "modified moving source"* in this limit. Such a result is also what one would anticipate for a source in a finite length jet, since the modified moving source merely requires a small neighborhood of fluid traveling with it. A second example[5] is a source in a jet, but at rest relative to the external air. This source is necessarily moving relative to the jet fluid, and is considered a modified moving source. Analyzed by infinite jet methods in the limit of zero frequency the result is a simple source radiating uniformly in all directions. This is again quite consistent with what one would expect for the finite jet in the zero frequency limit.

Another intuitive argument is obtained by approaching the finite jet problem (qualitatively) by modifying the boundary conditions for the infinitely long jet. Consider a jet of circular cross-section and, with the source as a center, construct a spherical surface which passes through the jet about one and one-half diameters upstream and downstream from the source. The portion of the sphere within the jet intercepts a solid angle which is five percent of the total for the sphere. It is within this limited angular range that the boundary conditions would have to be modified for the finite jet if uniform conditions are assumed over the three-diameter length. This suggests, though it certainly does not prove, that the radiation field outside the jet might not be seriously altered by the restriction of jet length.

It should be mentioned here that there is a region in which infinite-jet theory is definitely incorrect. This is a

---

*The modified moving source is defined and described in Ref. 5 and compared with the conventional moving source. The existence of other types of moving sources also is noted.

relatively small angular region in the far field near the jet axis. Here infinite-jet theory predicts mean-square pressures approaching zero at the axis, which would not be true for a real jet of finite length. Since the region is small and the pressures are ordinarily small we are not usually much concerned with this difficulty.

The preceding discussion may serve to indicate that intuitive arguments sometimes conflict and must be handled with caution. The range of conditions under which infinite-jet analysis is useful must be considered unknown at present.

Part 2 (retarded coordinates and transient sources)

The mean-square pressure for a sequence of transient sources contains an integral of the sum of the squared transmission coefficients over the entire frequency range (Eq. (27)). There is, however, a weighting factor in the integrand which, if each transient source goes through many cycles during its existence, becomes a delta-function. In this limit the mean-square pressure formula is much simplified (Eq. (28)), becoming independent of the transmission coefficients except at the basic frequency. A simple rule can then be used to obtain the mean-square pressure in retarded coordinates for the transient source sequence from that in source coordinates for a single permanent source: Make a formal transformation of the latter to retarded coordinates and multiply by $\left[1 + Mx_2/R\right]$. On examining Lighthill's work we found that his original result had been corrected by Ffowcs-Williams by applying a multiplicative factor of $[1 + Mx_2/R]$. If we assume that this corresponds to our transient source effect, then the Lighthill - Ffowcs-Williams result would be applicable in the limit when each transient quadrupole goes through many cycles.

It can readily be shown that, for a pulsating source at the center of the jet, the distance traveled downstream from the nozzle during one cycle is equal to the jet thickness divided by the Strouhal number. Thus if the Strouhal number, S_T, is 0.1 the source travels ten jet diameters in completing one cycle. For $S_T = 0.2$ the source completes a cycle while moving downstream five jet diameters. Thus for low S_T (or low frequency) it is difficult to justify the assumption that the transient source passes through many cycles. However, we have an equation (Eq. (27)) which provides for transient sources passing through a reduced number of cycles down to one cycle. In this equation is a factor which becomes a delta-function in the limit as $n \to \infty$:

$$\frac{2\,(\omega/\omega_0)^2 \sin^2(2\pi n\omega/\omega_0)}{\pi^2 n\,(\omega^2/\omega_0{}^2 - 1)^2} = F_\delta \qquad (109)$$

In Fig. 23 we examine this factor as a function of ω/ω_0 for two cycles ($n = 1$) and for one cycle ($n = \frac{1}{2}$). ($2n$ must be an integer.) Also, we examine a related factor, not derived here, which applies to half-cycles:

$$\frac{8\,(\omega/\omega_0)^2 \cos^2\left[\frac{1}{2}(m\pi\omega/\omega_0)\right]}{\pi^2 m\,(\omega^2/\omega_0{}^2 - 1)^2} = F_\delta{}' \qquad (110)$$

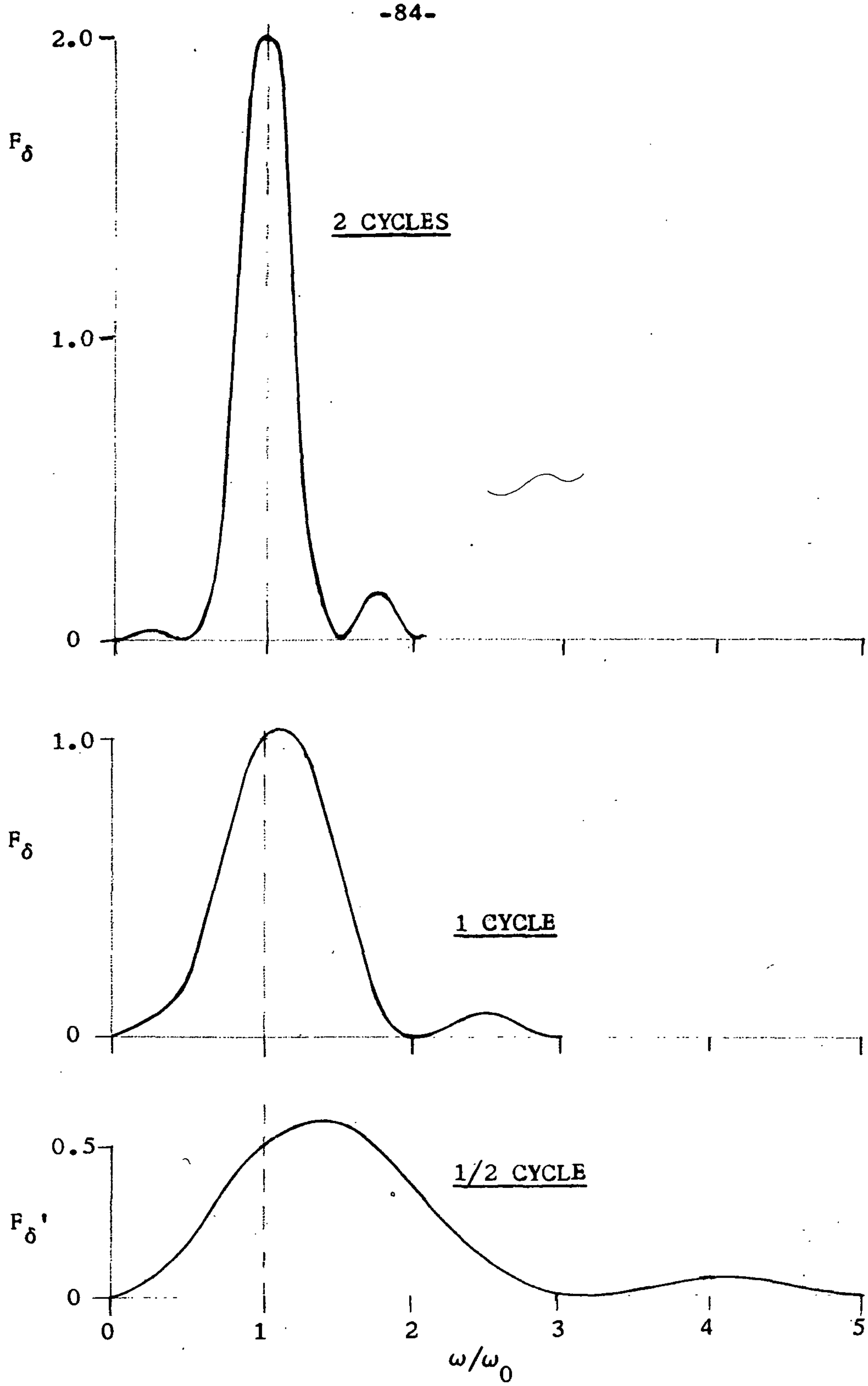

Fig. 23 PLOTS OF EQS. (109) AND (110)

(In Eq. (110) m must be odd, and m = 1 corresponds to one-half cycle.)

Fig. 23 suggests that, if the pulsating source passes through only one cycle or one-half cycle in its lifetime, the factor deviates materially from the delta-function. In some such cases the delta-function may still be an adequate approximation. In others it may be necessary to use the more general equation (Eq. (27)) instead of the simpler one (Eq. (28)) which applies when n approaches infinity. There may be an alternative way to define amplitude vs. frequency for the noise-generating sources, permitting use of the simpler equation in all cases, but that is beyond the scope of this study.

CONCLUSIONS

(1) The acoustical source traveling with the local fluid produces two types of disturbances. One we will term true sound, which consists of true waves carrying energy. The other we will call pseudo-sound (characterized by exponential decay in our analysis) which transmits energy only by interference with reflected waves. At a Mach number of zero all the far-field noise originates as true sound at the source. However at a Mach number as low as 0.3 most of the far-field noise originates as pseudo-sound at the source.

(2) A review of the methods for theoretically constructing quadrupoles in a shear layer suggests that there is no elementary reason for discarding dipole and source radiation in our analysis. If mean velocity varies across the jet, then the absence of any net source strength in the entire jet does not necessarily make source radiation unimportant. Similarly the absence of any net dipole strength does not result in purely quadrupole radiation.

The dominance of quadrupole radiation in jet noise appears to be a feature of Lighthill's simplified model of the jet, but it is not necessarily characteristic of real jets.

(3) Moving a source off the centerline of the jet generally has little effect on the noise radiated as long as the source remains within the central high-velocity region of the jet. However, a source of the same strength halfway

out in the shear layer has greatly reduced noise radiation (which is probably to be expected because of the reduced speed of convection).

(4) The noise radiated by sources on the centerline of circular cylindrical and two-dimensional jets is compared for similar velocity profiles, Mach numbers and jet thicknesses. The circular jet cases show pressure lobes which are broader and rotated in closer to the downstream jet axis. Also, the variation of far-field noise/(frequency)^2 with Strouhal number is greater for the circular jet. Here, source strength, defined as maximum volume introduced per unit time, is fixed.

(5) The effect of raising the jet temperature above ambient with fixed jet <u>velocity</u> and source strength is illustrated. The Mach number based on <u>ambient</u> temperature is 0.7 for the examples given, and Strouhal numbers up to 0.2 are considered. The major effects are a reduction in magnitude of the mean-square pressure, and rotation of the pressure lobes away from the downstream jet axis.

(6) A primary effect of changing from a source to a quadrupole (both on the centerline) is that pressure peaks generally rotate in towards the downstream jet axis (see Appendix).

Appendix: DIPOLES AND QUADRUPOLES IN A TWO-DIMENSIONAL JET

Equations for Mean-Square Pressure

In our previous reports[2-4] the acoustical source (i.e. monopole source) on the jet centerline has been taken as the noise generator. Since quadrupoles are frequently considered as the primary noise generators in a jet, we have extended the analysis to include dipoles (three types) and quadrupoles (six types), all located on the centerline of a two-dimensional jet. Only the results of the analysis will be given here. Details of the derivation are omitted since they follow the methods described earlier (see Section 2), methods which were developed for the source in Refs. 2-4 and which are applied in detail for the source in the shear layer in Section 4 of this report. Following are the expressions for far-field mean-square pressure ($\overline{\Delta p^2}$) for these singularities, including the source.

The source strength is here taken as the maximum volume per unit time introduced by the source. (Lighthill uses rate of change of mass flow as source strength.) A source strength factor A is defined such that source strength = $8\pi^2 A$. The corresponding dipole strength factor is then $A_d = A\ell$ where ℓ is the distance separating a source and a sink, each of strength $8\pi^2 A$. Similarly, the quadrupole strength factor is $A_q = A\ell^2$. $\overline{\Delta p_s{}^2}$ is the mean-square pressure produced by a source of unit strength factor.

source

$$\overline{\Delta p^2} = A^2\,\overline{\Delta p_s{}^2} = A^2\,\frac{2\pi^2\rho^2\omega^2}{R^2\,|1+Mx_2/R|^5}\,(z/R)^2\left[S''^2(\omega)+S'^2(\omega)\right] \qquad \text{(A-1)}$$

x-axis dipole

$$\overline{\Delta p^2} = \overline{\Delta p_s{}^2}\, A_d{}^2\, \omega'^2\, (x_2/R)^2/(1+Mx_2/R)^2 \tag{A-2}$$

y-axis dipole

$$\overline{\Delta p^2} = \overline{\Delta p_s{}^2}\, A_d{}^2\, \omega'^2\, (y/R)^2/(1+Mx_2/R)^2 \tag{A-3}$$

z-axis dipole

$$\overline{\Delta p^2} = \overline{\Delta p_s{}^2}\, A_d{}^2\, \omega'^2\, \frac{S_A{}''^2(\omega)+S_A{}'^2(\omega)}{S''^2(\omega)+S'^2(\omega)} \left| 1 - \frac{(x_2/R)^2+(y/R)^2}{(1+Mx_2/R)^2} \right| \tag{A-4}$$

x-x quadrupole

$$\overline{\Delta p^2} = \overline{\Delta p_s{}^2}\, A_q{}^2\, \omega'^4\, (x_2/R)^4/(1+Mx_2/R)^4 \tag{A-5}$$

y-y quadrupole

$$\overline{\Delta p^2} = \overline{\Delta p_s{}^2}\, A_q{}^2\, \omega'^4\, (y/R)^4/(1+Mx_2/R)^4 \tag{A-6}$$

z-z quadrupole

$$\overline{\Delta p^2} = \overline{\Delta p_s{}^2}\, A_q{}^2\, \omega'^4 \left[1 - \frac{(x_2/R)^2+(y/R)^2}{(1+Mx_2/R)^2} \right]^2 \tag{A-7}$$

x-y quadrupole

$$\overline{\Delta p^2} = \overline{\Delta p_s{}^2}\, A_q{}^2\, \omega'^4\, (x_2/R)^2\, (y/R)^2/(1+Mx_2/R)^4 \tag{A-8}$$

x-z quadrupole

$$\overline{\Delta p^2} = \overline{\Delta p_s{}^2}\, A_q{}^2\, \omega'^4\, \frac{S_A{}''^2(\omega)+S_A{}'^2(\omega)}{S''^2(\omega)+S'^2(\omega)}\, \frac{(x_2/R)^2}{(1+Mx_2/R)^2} \left| 1 - \frac{(x_2/R)^2+(y/R)^2}{(1+Mx_2/R)^2} \right| \tag{A-9}$$

y-z quadrupole

$$\overline{\Delta p^2} = \overline{\Delta p_s^2}\, A_q^2\, \omega'^4 \frac{S_A''^2(\omega)+S_A'^2(\omega)}{S''^2(\omega)+S'^2(\omega)} \frac{(y/R)^2}{(1+Mx_2/R)^2} \left| 1-\frac{(x_2/R)^2+(y/R)^2}{(1+Mx_2/R)^2} \right| \tag{A-10}$$

Here, ρ is the mass density of the ambient air, ω is the generating frequency of the transient singularities, and ω' is ω/c where c is the velocity of sound. x_2, y and z are respectively the streamwise, lateral and normal distances of the observation point from the noise-generating region of the plane jet, and $R = \sqrt{x_2^2+y^2+z^2}$. M is the Mach number of the transient sources (or dipoles or quadrupoles) relative to the ambient air.

S' and S'' are related to the in-phase and out-of-phase transmission coefficients for symmetrical disturbances of the jet[2] (zero normal displacement at the jet centerline). S_A' and S_A'' are similarly related to transmission coefficients for anti-symmetrical disturbances (zero pressure at the jet centerline). For all of these S-terms programmed computations are desirable. (Expressions for S',S'' were derived in Ref. 2. These and S_A', S_A'' follow as special cases (i.e. for $z_s = 0$) of coefficients derived in Section 4. Using the notation of Section 4, Eqs. (29), (30) and (32) in particular, we find that

$$S_A' = \pm \frac{\sqrt{(1-M_sK_1)^2-K^2}\,\left[3B(1-M_sK_1)\right]\left[f(\zeta_1)[\;]_g-g(\zeta_1)[\;]_f\right]}{\text{Den.}}$$

$$S_A'' = -\frac{3B(1-M_sK_1)\left[f_\zeta(\zeta_1)[\;]_g-g_\zeta(\zeta_1)[\;]_f\right]}{\text{Den.}} \tag{A-11}$$

where the [illegible]$_f$, [illegible]$_g$ values of Eq. (22) are needed here. These also enter the denominator term, Den., Eq. (25).)

Discussion of Equations

Of the nine additional noise generators considered here, five (those involving only x and y axes) can be obtained by differentiation of the source far field. Three of the remaining four require anti-symmetric transmission coefficients, and the fourth (the z-z quadrupole) retains symmetric transmission coefficients but is not obtained by simple differentiation in the far field.

Since for the two-dimensional jet we are examining primarily the $\overline{\Delta p^2}$ in the plane $y = 0$, we are not now concerned with singularities having a y-axis. Also, we are more interested in quadrupoles than in dipoles, and this leaves the x-x, z-z and x-z quadrupoles for our attention. For simplicity, we consider now the x-x and z-z longitudinal quadrupoles and show in Fig. 24 the sum of the $\overline{\Delta p^2}$ values for these two (Eq. (A-5) plus Eq. (A-7)). (If they were assumed to pulsate in phase a source-like $\overline{\Delta p^2}$ would result.)

Fig. 25 shows for comparison purposes the $\overline{\Delta p^2}$ for a source (Eq. (A-1)).

Discussion of Figures

These figures show radial plots of $\overline{\Delta p^2}$ for jet Mach numbers 0.3 and 0.7, for a source and for the $[(x\text{-}x)+(z\text{-}z)]$ quadrupole (both located on the jet centerline in a jet with linear shear layers extending in to the centerline). The Strouhal

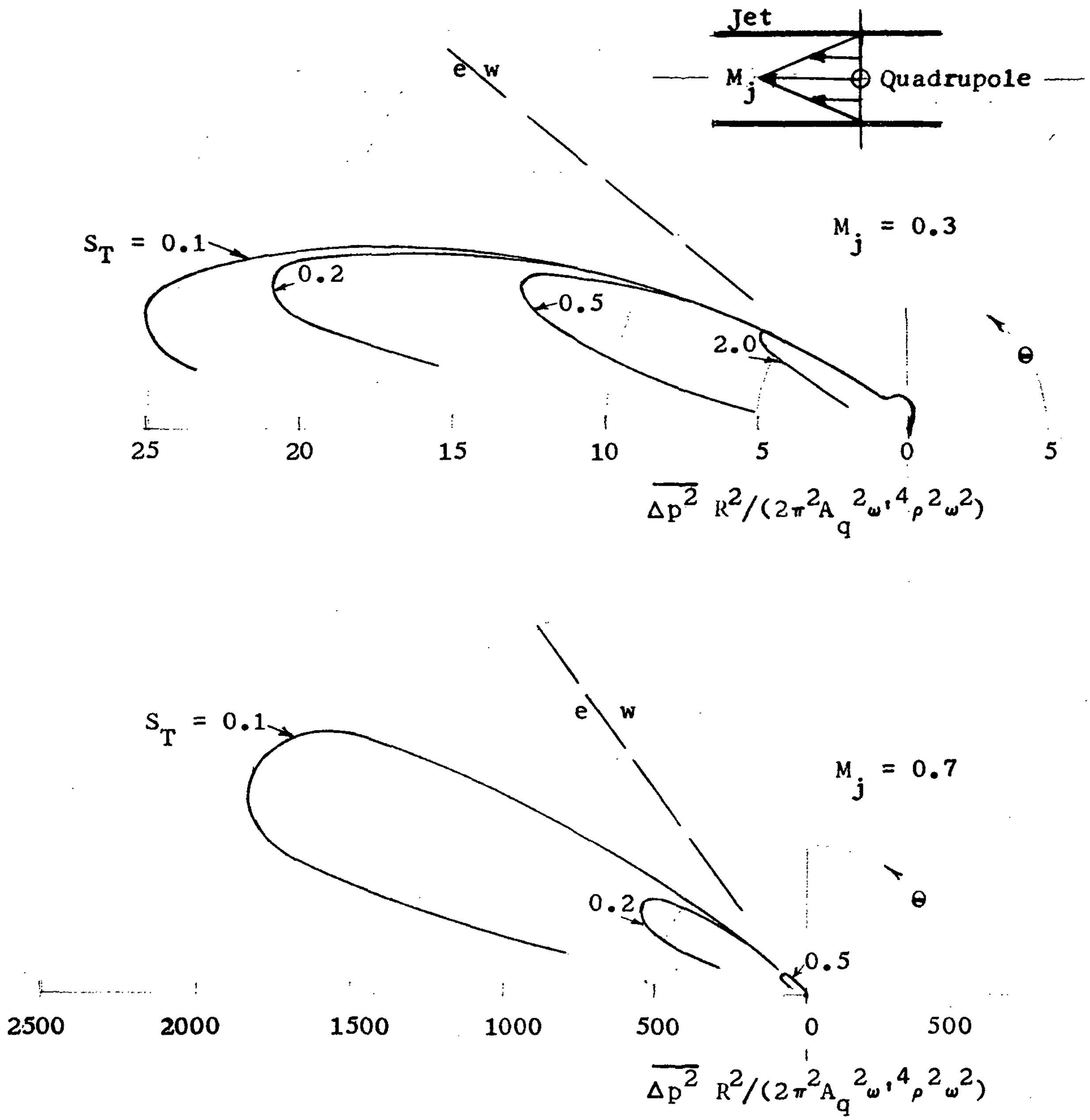

Fig. 24 MEAN-SQUARE PRESSURE IN THE FAR FIELD (POLAR PLOT):
$\overline{\Delta p^2}$(x-x quadrupole) + $\overline{\Delta p^2}$(z-z quadrupole).
Quadrupole at centerline; maximum jet Mach numbers
0.3 and 0.7

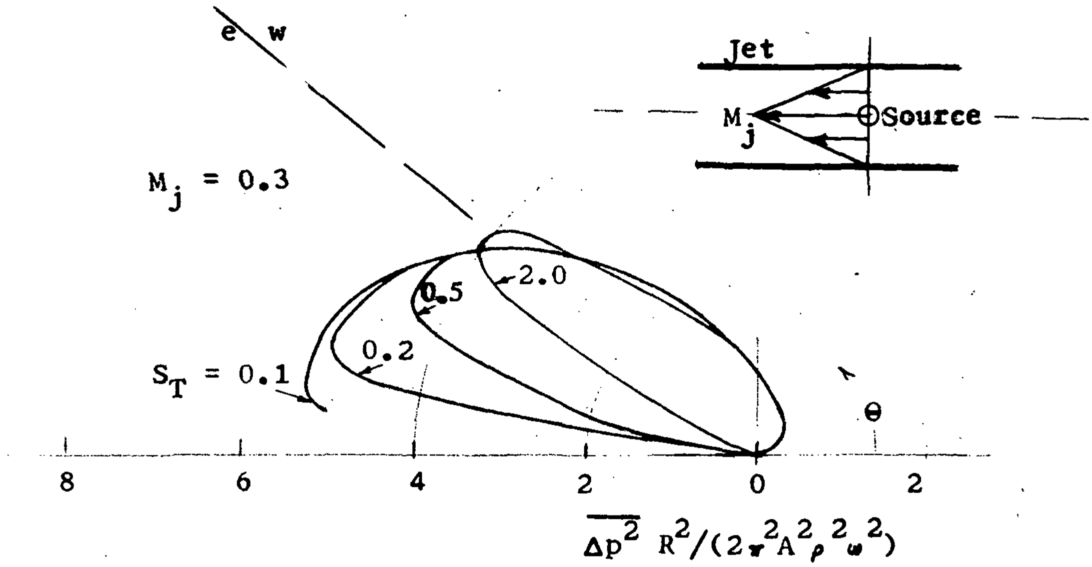

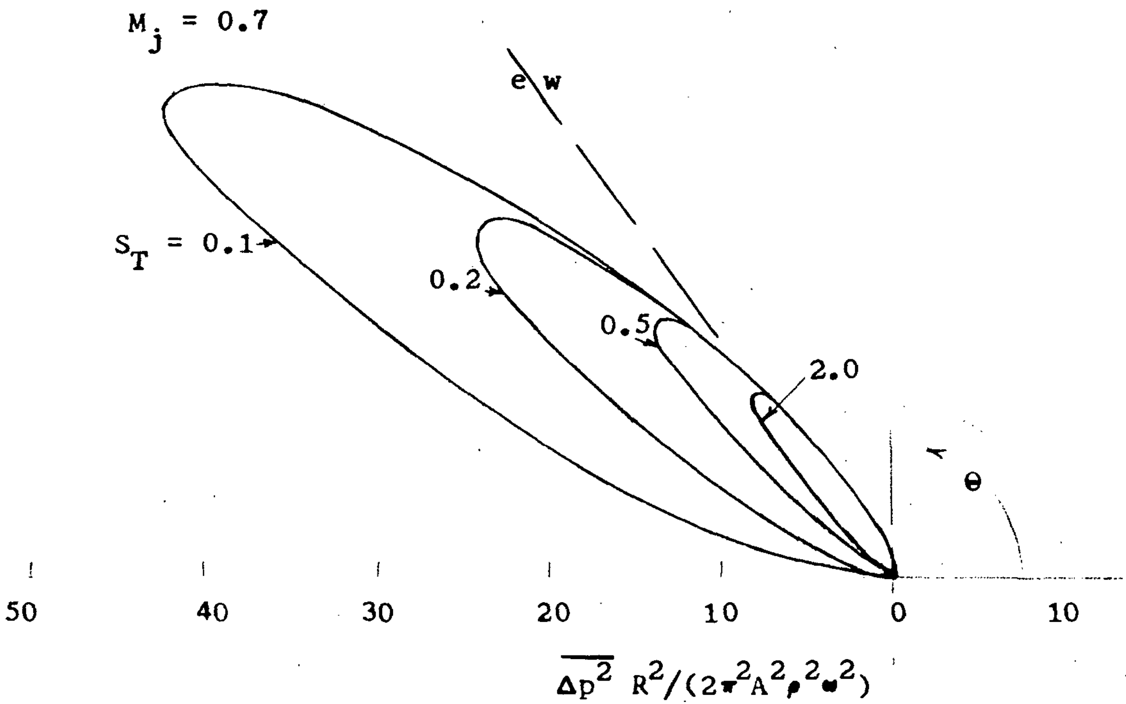

Fig. 25 MEAN-SQUARE PRESSURE IN THE FAR FIELD (POLAR PLOT): Source at centerline; maximum jet Mach numbers 0.3 and 0.7.

number, S_T, is defined as

$$S_T = (\omega/2\pi)(\text{jet thickness})/(\text{jet velocity})$$

where ω is the source or quadrupole frequency. Results are shown for S_T = 0.1, 0.2, 0.5 and 2.0. The radial line with e on one side and w on the other indicates the boundary between the region in which the disturbances leaving the singularity might be termed "pseudo-sound" and are exponentially decaying in z (e) and the region in which disturbances leaving the singularity are "true sound", or true waves (w). At a Mach number of zero all far-field noise is produced by disturbances which leave the noise generator as true sound. However, as noted in other examples, at a Mach number of only 0.3 most of the far-field noise is produced by disturbances originating as pseudo-sound.

The amplitudes for $\overline{\Delta p^2}$ are of interest (at present) only for comparing like Strouhal numbers at different Mach numbers for a given type of noise generator. It can be seen that for a fixed strength of the noise generator $\overline{\Delta p^2}$ rises rapidly with increasing Mach number. Before attempting to construct a power law for noise level as a function of Mach number other factors must be considered. For example, the dependence of noise generator strength on Mach number, the possibility that noise generator type depends on Mach number, the conversion of generating frequency to observed frequency, the contributions of various portions of the jet (which travel at different velocities) are some of these factors.

A primary effect of changing from sources to quadrupoles is that the pressure peaks generally rotate in towards the downstream axis.

References

1. Graham, E. W. and Graham, B. B.: Effect of a Shear Layer on Plane Waves of Sound in a Fluid. J. Acoustical Soc. Am. 46, pp. 169-175, 1969.

2. Graham, E. W. and Graham, B. B.: The Acoustical Source in a Two-Dimensional Jet. Boeing Sci. Res. Labs. Doc. D1-82-0909, 1969.

3. Graham, E. W. : A Sequence of Transient Acoustical Sources in an Idealized Jet. Boeing Sci. Res. Labs. Doc. D1-82-1002, 1970.

4. Graham, E. W. and Graham, B. B.: Transient Acoustical Sources in an Idealized Jet. J. Acoustical Soc. Am. 52, pp. 221-226, 1972.

5. Graham, E. W. and Graham, B. B.: A Note on Theoretical Acoustical Sources in Motion. J. Fluid Mech. 49, pp. 481-488, 1971.

6. Lighthill, M. J.: Sound Generated Aerodynamically. The Bakerian Lecture, 1961. Published in Proc. Roy. Soc. A267, pp. 147-182, 1962.

7. Landau, L. D. and Lifshitz, E. M.: Fluid Mechanics. Pergamon Press, 1959.

8. Lamb, H.: Hydrodynamics. Dover Publications, 1945, Sixth edition.

9. Magnus, W. and Oberhettinger, F.: Formulas and Theorems for the Special Functions of Mathematical Physics. Chelsea Publishing Company, 1949.

10. Blokhintsev, D. I.: Acoustics of a Non-Homogeneous Moving Medium. NACA T.M. 1399, 1946.

NASA-Langley, 1974 CR-2390

NATIONAL AERONAUTICS AND SPACE ADMINISTRATION
WASHINGTON, D.C. 20546

OFFICIAL BUSINESS
PENALTY FOR PRIVATE USE $300

SPECIAL FOURTH-CLASS RATE
BOOK

POSTAGE AND FEES PAID
NATIONAL AERONAUTICS AND
SPACE ADMINISTRATION
451

U.S.MAIL

POSTMASTER: If Undeliverable (Section 158 Postal Manual) Do Not Return

"The aeronautical and space activities of the United States shall be conducted so as to contribute . . . to the expansion of human knowledge of phenomena in the atmosphere and space. The Administration shall provide for the widest practicable and appropriate dissemination of information concerning its activities and the results thereof."

—NATIONAL AERONAUTICS AND SPACE ACT OF 1958

NASA SCIENTIFIC AND TECHNICAL PUBLICATIONS

TECHNICAL REPORTS: Scientific and technical information considered important, complete, and a lasting contribution to existing knowledge.

TECHNICAL NOTES: Information less broad in scope but nevertheless of importance as a contribution to existing knowledge.

TECHNICAL MEMORANDUMS: Information receiving limited distribution because of preliminary data, security classification, or other reasons. Also includes conference proceedings with either limited or unlimited distribution.

CONTRACTOR REPORTS: Scientific and technical information generated under a NASA contract or grant and considered an important contribution to existing knowledge.

TECHNICAL TRANSLATIONS: Information published in a foreign language considered to merit NASA distribution in English.

SPECIAL PUBLICATIONS: Information derived from or of value to NASA activities. Publications include final reports of major projects, monographs, data compilations, handbooks, sourcebooks, and special bibliographies.

TECHNOLOGY UTILIZATION PUBLICATIONS: Information on technology used by NASA that may be of particular interest in commercial and other non-aerospace applications. Publications include Tech Briefs, Technology Utilization Reports and Technology Surveys.

Details on the availability of these publications may be obtained from:

SCIENTIFIC AND TECHNICAL INFORMATION OFFICE

NATIONAL AERONAUTICS AND SPACE ADMINISTRATION

Washington, D.C. 20546

NATIONAL AERONAUTICS AND SPACE ADMINISTRATION
WASHINGTON, D.C. 20546

OFFICIAL BUSINESS
PENALTY FOR PRIVATE USE $300

SPECIAL FOURTH-CLASS RATE
BOOK

POSTAGE AND FEES PAID
NATIONAL AERONAUTICS AND
SPACE ADMINISTRATION
451

U.S. MAIL

POSTMASTER : If Undeliverable (Section 158 Postal Manual) Do Not Return